1960

Dispersion of ultrasound in ethanes, ethylene, and methanes

Leonard Maurice Valley
Iowa State University

Mic 60-4907

VALLEY, Leonard Maurice. DISPERSION OF ULTRASOUND IN ETHANES, ETHYLENE, AND METHANES.

Iowa State University of Science and Technology
Ph.D., 1960
Physics, general

University Microfilms, Inc., Ann Arbor, Michigan

DISPERSION OF ULTRASOUND IN ETHANES, ETHYLENE, AND METHANES

by

Leonard Maurice Valley

A Dissertation Submitted to the
Graduate Faculty in Partial Fulfillment of
The Requirements for the Degree of
DOCTOR OF PHILOSOPHY

Major Subject: Physics

Approved:

Signature was redacted for privacy.

In Charge of Major Work

Signature was redacted for privacy.

Head of Major Department

Signature was redacted for privacy.

Dean of Graduate College

Iowa State University
Of Science and Technology
Ames, Iowa

1960

TABLE OF CONTENTS

I. INTRODUCTION

The idea that, when a sound wave passes through a gas, the molecules might relax at sufficiently high frequencies was put forward by Jeans (12). The dispersion of sound which results from this relaxation was discovered by Pierce (22) in 1925. The frequency of the sound wave in the gas is increased until it reaches the dispersive region where the velocity of the sound begins to increase. Above this dispersive region the velocity again becomes constant and assumes the value predicted by the specific heat theory of gases with no vibrational contribution.

Herzfeld and Rice (10) explained this effect on the hypothesis that molecular vibrations require a relatively large number of collisions to return to thermal equilibrium as compared to molecular rotations and translations. This was further verified when Dwyer (6) looked at the spectrum of I_2 gas after it had been excited to higher vibrational levels. The transfer of energy into or out of the vibrational degrees of freedom of a molecule is indeed a slow process. Such a transfer of energy can be considered as a relaxation phenomenon. The relaxation time for such a phenomenon is defined as the time necessary for a disturbance from equilibrium to fall to 1/e of its original value.

The transmission of a high frequency sound wave through a gas is accompanied by rapid changes in temperature, and

as the frequency increases a range is reached in which the transfer of thermal energy into and out of the vibrational degrees of freedom cannot keep pace with the acoustic cycle. (The thermal energy of translation and rotation can still follow the acoustic cycle in this range.) This results in a vibrational heat capacity lag and at high enough frequencies the sound wave will see only a specific heat due to the translational and rotational degrees of freedom.

The velocity of propagation of sound in a gas depends upon the specific heat, and it is clear now that the specific heat is a function of the relaxation time of the vibrational degrees of freedom and the frequency of the sound wave. Therefore the vibrational relaxation time for a gas can be determined by measuring the frequency dependence of the velocity of sound in the gas.

Theoretical predictions of relaxation times have been made and compared with experimental values. The most recent quantum mechanical theory gives good agreement with experiment in many cases. However, such theories are very complex and necessarily require several assumptions which restrict the validity of the theoretical results.

If more than one vibrational degree of freedom is present, there may also be more than one relaxation time. This makes the problem even more complex. One might expect to see such an effect in some polyatomic molecules or in

mixtures of two gases each characterized by a single relaxation time.

A very thorough study of many diatomic and triatomic molecules was carried out in the years following the discovery by Pierce (22). In the last six or seven years a great deal of work has been done on more complex gases. In particular, the halogen substituted methane derivatives have received an intensive examination. This was followed by work on ethylene derivatives, some ethane derivatives and other complex molecules. It was found that all of these gases except CH_2Cl_2 and possibly CO_2 could be considered to have a single relaxation time. Also, the few mixtures which were investigated show only single dispersion.

It is evident that more investigations leading to information about multiple dispersion might be very fruitful. With the capacity to reach higher frequencies it is logical to investigate thoroughly the ethane derivatives as well as certain mixtures which may show multiple dispersion. It is the purpose of this dissertation to report the experimental and theoretical results of such an investigation.

II. THEORETICAL CONSIDERATIONS

A. Velocity of Sound

1. Low frequency region

In the low frequency region (when the frequency is below that value for which the velocity starts to increase with frequency) the propagation equation is very simple. Richards (24) derives the equation for the velocity of a plane sound wave in a homogeneous isotropic medium,

$$V^2 = \left(\frac{\partial P}{\partial \rho}\right)_T + \left(\frac{\partial P}{\partial T}\right)_\rho^2 \cdot \left(\frac{MT}{C\rho^2}\right) \quad ; \qquad (1)$$

V is the velocity of sound, P the pressure, ρ the density, T the absolute temperature, M the molecular weight, and C the specific heat at constant volume (all specific heats will be given at constant volume unless otherwise stated). It was assumed for Eq. (1) that the sound wave is transmitted adiabatically but this is a justifiable assumption.

For an ideal gas $P = RT\rho/M$ where R is the universal gas constant. Using this in Eq. (1) we get

$$V_o^2 = \frac{RT}{M}\left(1 + \frac{R}{C_o}\right) \qquad (2)$$

where V_o is the velocity of sound in an ideal gas and C_o is the specific heat in the low frequency region.

2. Dispersive region

Pierce (22) discovered in 1925 that the velocity of sound in carbon dioxide is a function of frequency. This dispersion could be explained by Eq. (1) if the specific heat were a function of frequency.

Herzfeld and Rice (10) hypothesized that there is a slow rate of energy transfer between the external and internal degrees of freedom which keeps the internal degrees of freedom from taking their share of heat during an acoustic cycle and therefore the sound wave sees an effective specific heat, C_ω, which decreases from C_o as the frequency is increased. This decrease in the specific heat would cause an increase in the velocity which is what Pierce (22) observed.

For the dispersive region the velocity of sound in an ideal gas would be written:

$$V^2_{(\omega)} = \frac{RT}{M}\left(1 + \frac{R}{C_\omega}\right) \quad , \tag{3}$$

where C_ω is the specific heat of the gas as a function of frequency.

Neglecting electronic excitation, C_o is made up of contributions from translational, rotational, and vibrational degrees of freedom:

$$C_o = C_{trans} + C_{rot} + C_{vib} \quad . \tag{4}$$

As suggested by Herzfeld and Rice (10) a decrease in the effective specific heat with an increase in frequency of the sound wave is seen because the energy transfer into the internal degrees of freedom (rotation and vibration) lags behind the acoustic cycle. It was believed that the vibrational degrees of freedom would have a slower rate of energy transfer than the rotational degrees of freedom and this was verified by Dwyer (6) for I_2. So, C_{vib}, the specific heat of vibration will be the first to lag and it is with this heat capacity lag that this dissertation will be concerned.

In single dispersion the specific heat will go from C_o to $C_o - C_{vib}$ in a single smooth step as the frequency is increased through the dispersive region. C_∞, the specific heat at high frequencies is defined as

$$C_\infty \equiv C_o - C_{vib} = C_{trans} + C_{rot} \quad . \tag{5}$$

From Richards (24) one has, if the vibrational degrees of freedom are characterized by a single relaxation time,

$$C_\omega = C_\infty + \frac{C_{vib}}{1 + i\omega\theta} \tag{6}$$

where θ is the vibrational relaxation time and $\omega = 2\pi f/p$ (f/p is the frequency in cycles per second at one atmosphere - see page 32). Substituting this into Eq. (3) one finds, keeping the real part,

$$V^2_{(\omega)} = \frac{RT}{M}\left(1 + R\,\frac{C_o + \omega^2\theta^2 C_\infty}{C_o^2 + \omega^2\theta^2 C_\infty^2}\right) . \tag{7}$$

This is the velocity of sound as a function of frequency for an ideal gas showing single dispersion. It has been assumed that the frequency of the sound wave is not yet high enough to cause any lag in the rotational or translational specific heats. The velocity of sound at high frequencies (that is frequencies above the vibrational dispersive region but below the rotational or translational dispersive regions) is given by

$$V^2_\infty = \frac{RT}{M}\left(1 + \frac{R}{C_\infty}\right) . \tag{8}$$

The inflection frequency of Eq. (7) is easily found by differentiation to be

$$f_i = \frac{C_o}{2\pi\theta C_\infty} . \tag{9}$$

Experimental determination of f_i allows one to calculate the vibrational relaxation time,

$$\theta = \frac{C_o}{2\pi f_i C_\infty} \quad . \tag{10}$$

If a complex molecule shows single dispersion it is assumed that all energy exchanges between vibration and translation are through an exchange mode. The internal exchanges are assumed to have very short relaxation times.

Taking into account that the specific heat of the exchange mode is only a part of the total specific heat of vibration, the relaxation time of the exchange mode is

$$\theta_e = \frac{C_e}{C_{vib}} \theta \tag{11}$$

where C_e is that portion of C_{vib} associated with the exchange mode.

3. Double dispersion

Double dispersion here refers to the case in which the specific heat will go from C_o to $C_o - C_{vib}$ in two steps. The dispersion is then characterized by two relaxation times, θ_1 and θ_2, and the vibrational specific heat is $C_{vib} = C_1 + C_2$. The subscript one refers to the first step in the V^2 vs

f/P plot and the subscript two to the second step. C_2 is the specific heat of the hindered mode of rotation in all the cases considered in this dissertation. C_1 is the specific heat of the other modes of vibration or what shall be called the "regular" vibrations.

From Richards (24),

$$C_\omega = C_\infty + \frac{C_1}{1 + i\omega\theta_1} + \frac{C_2}{1 + i\omega\theta_2} \tag{12}$$

for the double dispersion case. Substituting this into Eq. (3) we get the equation for the velocity of sound in an ideal gas which shows double dispersion:

$$V^2_{(\omega)} = \frac{RT}{M}\left(1 + R\,\frac{C_o + \omega^2 A + \omega^4 B}{C_o^2 + \omega^2 D + \omega^4 E}\right) \tag{13}$$

where:

$$A \equiv C_\infty \theta_1^2 + C_2\theta_1^2 + C_\infty \theta_2^2 + C_1\theta_2^2$$

$$B \equiv C_\infty \theta_1^2\theta_2^2$$

$$D \equiv C_\infty^2 \theta_1^2 + C_\infty^2 \theta_2^2 + 2C_\infty C_2\theta_1^2 + C_2^2\theta_1^2 + 2C_\infty C_1\theta_2^2 + C_1^2\theta_2^2 + 2C_1C_2\theta_1\theta_2$$

$$E \equiv C_\infty^2 \theta_1^2\theta_2^2 \quad .$$

It is felt that Eq. (13) should be used in analyzing the data of gases in which double dispersion is observed. Others have attempted to use a combination of two single dispersion curves but this is satisfactory in only a few special cases.

In Figure 1, a comparison of the two approaches is given. For a given gas, values of Θ_1 and Θ_2 are assigned and $V^2_{(\omega)}$ from Eq. (13) is calculated and plotted. Similarly, for the same gas, same conditions, and same Θ_1 and Θ_2; single dispersion curves from Eq. (7) are plotted for each step. Now if the dispersion of the second step is added to the $V^2_{(\omega)}$ of the first step at given values of f/p one gets the combination of the two single dispersion curves mentioned above. The difference in the two methods is very evident and significant. The important thing to notice, however, is the difference which occurs in the first step. The single dispersion combination results predict that the double dispersion curve should be higher in the first step than the single dispersion curve for that step. A look at the double dispersion curve of Eq. (13) shows that it is actually lower in the first step as well as in the second step.

This suggests that there is a fairly strong interaction between the two relaxation phenomena which is completely neglected by the single dispersion combination results. In A, B, D, and E of Eq. (13) appear the many cross terms

Figure 1. Velocity dispersion in C_2H_6 by three methods of calculation

———— double dispersion Eq. (13)
——.—— single dispersion Eq. (7)
- - - - I-single dispersion for first step, II-single dispersion for second step, III-combination of I and II.
Insert: to show clearly that the double dispersion curve is lower even in the first step.

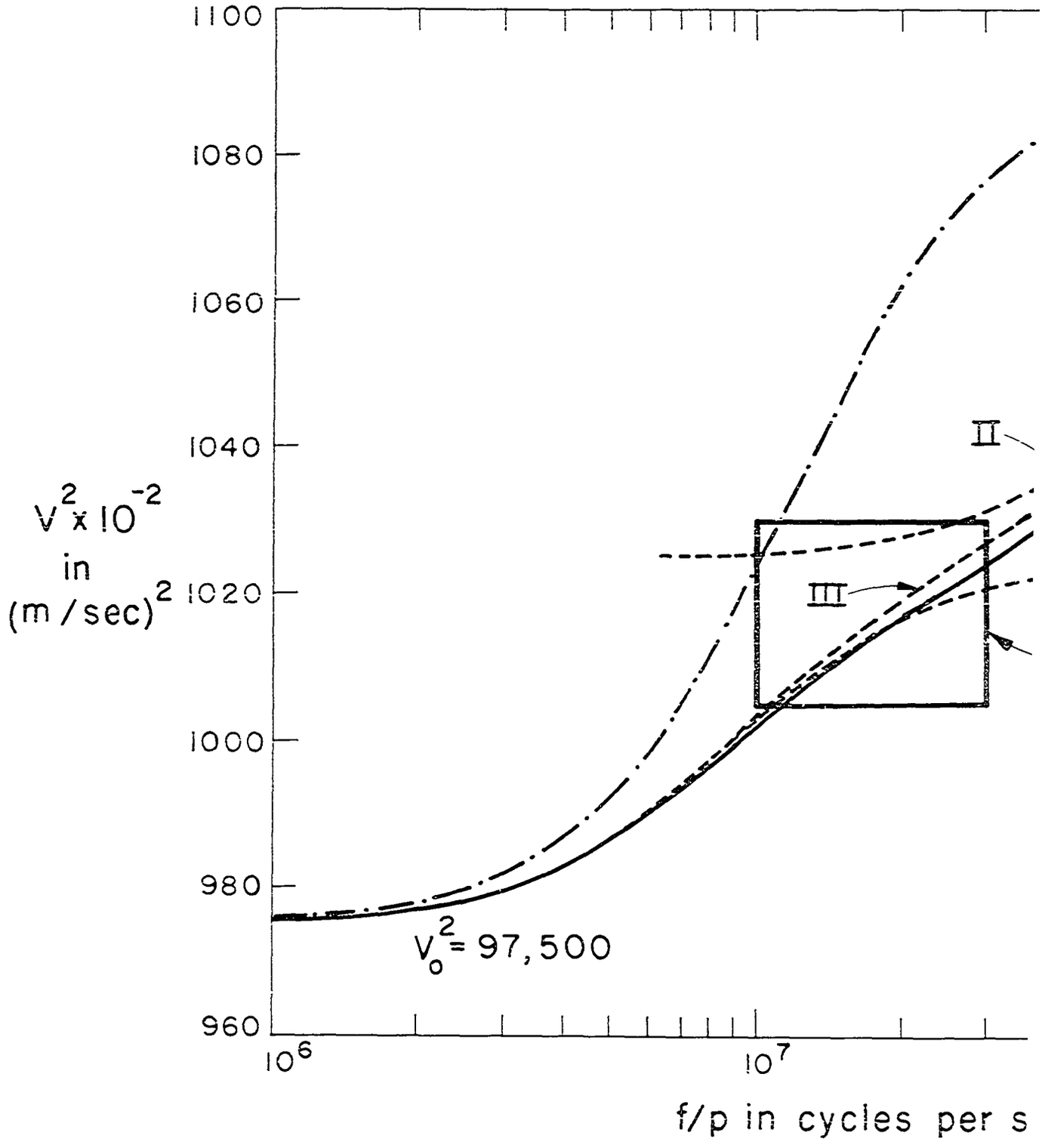
1100
1080
1060
1040
1020
1000
980
960
$V^2 \times 10^{-2}$
in
$(m/sec)^2$
$V_o^2 = 97,500$
II
III
10^6
10^7
f/p in cycles per s

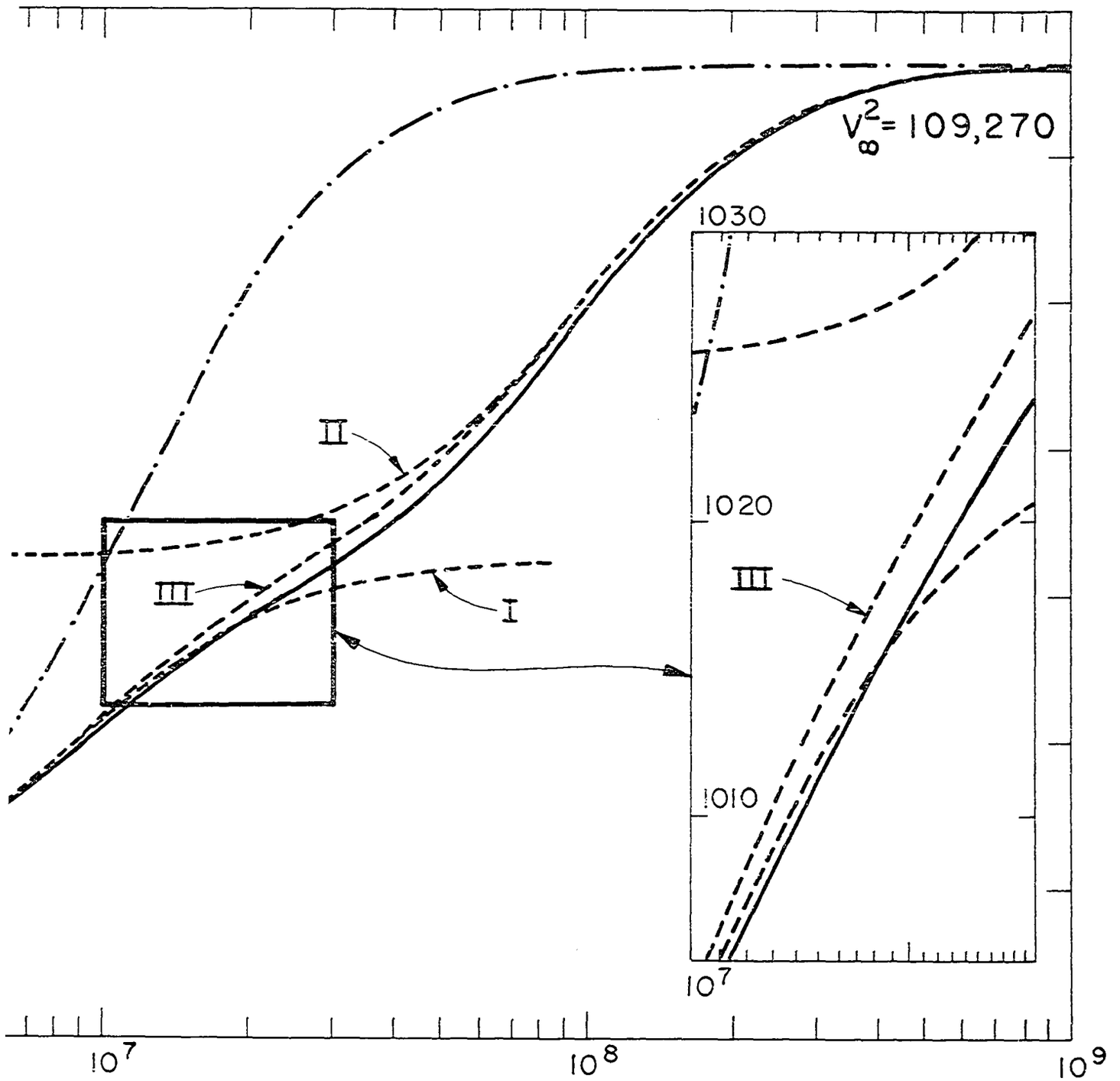
$V_\infty^2 = 109{,}270$
1030
1020
1010
10^7
II
III
I
III
10^7
10^8
10^9
f/p in cycles per second-atmosphere

which determine the strength of this interaction. The data for double dispersion fit the curve of Eq. (13) very well also and this will be considered in the proper section.

4. Correction to ideal

The use of the dispersion equations requires that the experimental results be idealized. Sette et al. (31) give the following relation between V_r, the real velocity, and V_i, the ideal velocity,

$$\frac{V_r}{V_i} = 1 - \alpha P \tag{14}$$

where

$$\alpha \equiv -\left[\frac{B}{RT} + \frac{1}{C_o}\left(\frac{dB}{dT} + \frac{RT}{2C_o^p} \cdot \frac{d^2B}{dT^2}\right)\right]$$

and P is the pressure, B the second virial coefficient, and C_o^p the specific heat at constant pressure for low frequencies.

The second virial coefficient may be calculated by using the Berthelot relation:

$$B = \frac{9}{128} \cdot \frac{RT_c}{P_c}\left(1 - \frac{6T_c^2}{T^2}\right) \tag{15}$$

where T_c is the critical temperature and P_c the critical pressure. If critical data are not available, the critical constants may be calculated by the method of Meissner and Redding (20).

The second virial coefficient for mixtures is calculated using Eq. (15) where T_c and P_c are the critical constants for the mixture. The standard method for calculating T_c and P_c is used. The critical temperature for a mixture is

$$T_c = T_c^A (1 - \chi) + T_c^B \chi \qquad (16)$$

where T_c^A is the critical temperature of gas A, T_c^B the critical temperature of gas B, and χ the mole fraction of gas B present. Similarly, the critical pressure for the mixture is

$$P_c = P_c^A (1 - \chi) + P_c^B \chi \quad . \qquad (17)$$

5. Determination of specific heats

The equipartition theorem states that in a system in equilibrium each degree of freedom of a molecule, which has one square term in the energy, possesses an amount of energy $\frac{1}{2}kT$ where k is Boltzmann's constant and T the absolute temperature. The translational energy per molecule is therefore

$\frac{3}{2}kT$ and the rotational (kinetic) energy is $\frac{3}{2}kT$ for a nonlinear molecule (symmetrical or nonsymmetrical). This classical theorem may be used because the energies are effectively classical for room temperature or above. Therefore, the specific heat per molecule due to translation and rotation is 3k or the specific heat per mole is

$$C_{\infty} = 3R \quad . \tag{18}$$

The vibrational energy has two square terms (potential and kinetic) in the energy based upon the simple harmonic oscillator. Therefore the vibrational energy is kT per degree of freedom and the specific heat is k if the vibrational contribution is fully realized. This, however, is not the case.

The total contribution to the specific heat for n modes of vibration is given by the Planck-Einstein equation (38):

$$C_{vib} = \sum_{i=1}^{n} \frac{\ell_i R \left(\frac{h\nu_i}{kT}\right)^2}{2\left[\cosh\left(\frac{h\nu_i}{kT}\right) - 1\right]} \; ; \tag{19}$$

ν_i is the frequency of the i^{th} mode of vibration and ℓ_i is the degeneracy of the i^{th} mode. In Eq. (19) it is assumed that one has harmonic oscillators. Since the actual levels

are not evenly spaced, as was assumed, there will be a slight error in using Eq. (19). This error is, for this work, usually considerably less than one per cent.

Eq. (19) does not hold for a mode of vibration caused by hindered rotation in the molecule. So for ethane type molecules C_o must be found some other way. If good low frequency data for V_o are available one can use Eq. (2) to find C_o. This method was used whenever C_{vib} could not be found using Eq. (19).

In the case of double dispersion, it is necessary to use a combination of the two methods mentioned above. The relationship

$$C_1 + C_2 = C_o - 3R = C_{vib} \qquad (20)$$

is used. C_o is found by using the low frequency data and C_1 is calculated using Eq. (19). Eq. (20) is solved for C_2 and thus all the specific heat information necessary for the use of Eq. (13) is known.

6. Mixtures

If a mixture of two gases, A and B, each separately characterized by a single relaxation time, exhibits single dispersion Eq. (7) may be used to analyze the data. The only difference for such mixtures is that one must determine

an effective molecular weight, M_{eff}, and an effective specific heat for low frequencies, $(C_o)_{eff}$.

For a mixture which has mole fraction χ of gas B one has

$$M_{eff} = M_A(1 - \chi) + M_B\chi \tag{21}$$

where M_A is the molecular weight of gas A and M_B is the molecular weight of gas B. Also:

$$\left(C_o\right)_{eff} = \left(C_o\right)_A (1 - \chi) + \left(C_o\right)_B \chi \tag{22}$$

where $\left(C_o\right)_A$ is the low frequency specific heat for gas A and $\left(C_o\right)_B$ is the low frequency specific heat for gas B. The procedure is then straight forward.

If a mixture of two gases exhibits double dispersion, Eq. (13) must be used. Let us look at the case in which gas A alone has a single relaxation time and gas B alone has two relaxation times. M_{eff} is determined by Eq. (21) and $\left(C_o\right)_{eff}$ by Eq. (22). However, the constants A, B, D, and E of Eq. (13) will depend upon $\left(C_1\right)_{eff}$ and $\left(C_2\right)_{eff}$, the effective specific heats for each step in the double dispersion curve.

For the mixtures considered here, the first step in the dispersion curve is determined by $\left(C_{vib}\right)_A$, the vibrational specific heat of gas A and C_1 of gas B. Therefore

$$\left(C_1\right)_{eff} = \left(C_{vib}\right)_A (1 - \chi) + C_1\chi \quad . \qquad (23)$$

χ is again the mole fraction of gas B present. $\left(C_2\right)_{eff}$ will then be:

$$\left(C_2\right)_{eff} = C_2\chi \quad . \qquad (24)$$

Here C_2 is the vibrational specific heat of the second step of the dispersion curve for gas B alone. One can then use Eq. (13) to find the relaxation times for the mixtures being examined.

B. Relaxation Theory

1. Collision lifetimes

One would like a relationship between the collision rate and the relaxation time. The relaxation time Θ is the observed quantity and from this one should be able to calculate the collision lifetime, Z_{10}. Z_{10} is the number of collisions per de-excitation from the first excited state to the ground state.

Two cases will be treated here, the two-state case and the simple harmonic oscillator case. The two-state case gives a clear picture of the problem involved but the simple harmonic oscillator case gives the more accurate result.

In the two-state case one assumes that there are n molecules of the gas present, n_1 of these in the first excited state and n_0 in the ground state ($n = n_1 + n_0$). The time rate of change of n_1 is then:

$$\frac{dn_1}{dt} = k_{01} n_0 - k_{10} n_1 \tag{25}$$

where k_{01} is the average number of $0 \rightarrow 1$ transitions per ground state molecule per second and k_{10} is the average number of $1 \rightarrow 0$ transitions per excited molecule per second.

Eq. (25) can easily be solved for n_1 to get:

$$n_1 = A + B \exp\left(- k_{01} - k_{10}\right) t$$

where A and B are constants. Therefore the relaxation time of this process is

$$\Theta = \frac{1}{k_{10} + k_{01}} \quad . \tag{26}$$

Now let us look at the simple harmonic oscillator case. Herzfeld and Litovitz (9) discuss this quite thoroughly. It is assumed that there are an infinite number of states j and that transitions are possible only for $\Delta j = \pm 1$. Therefore the time rate of change of the number of particles in the j^{th} state is

$$\frac{dn_j}{dt} = k_{j-1,j}n_{j-1} - k_{j,j-1}n_j + k_{j+1,j}n_{j+1} - k_{j,j+1}n_j \quad (27)$$

Proceeding from this in a manner slightly more involved than for the two-state case one finds

$$\Theta = \frac{1}{k_{10} - k_{01}} \quad . \quad (28)$$

Note a change in sign from Eq. (26).

It is known that $k_{01} = k_{10}\ell \exp(-\epsilon/kT)$ where ℓ is the ratio of the statistical weight of the excited state to the statistical weight of the ground state, ϵ is the energy gap between the two states, k is the Boltzman constant, and T is the absolute temperature of the gas. For the simple harmonic oscillator $\epsilon = h\nu$ and ℓ is unity.

Therefore, one has for the two-state case with $\ell = 1$,

$$\Theta = \frac{1}{k_{10}\left[1 + \exp(-\epsilon/kT)\right]} \quad (26a)$$

and for the simple harmonic oscillator:

$$\Theta = \frac{1}{k_{10}\left[1 - \exp(-h\nu/kT)\right]} \quad . \quad (28a)$$

If the temperature is so low that only the two lowest states

need be considered, the expression in brackets reduces to unity for both Eq. (26a) and Eq. (28a) and the result is $\Theta = 1/k_{10}$. If the temperature is not this low then Eq. (26a) is not applicable and Eq. (28a) is the equation to use.

We will be concerned here with Eq. (28a). If the collision rate per molecule is K and if the probability per collision that a de-excitation will occur is P_{10}, then $k_{10} = K P_{10}$. Collision lifetimes, $Z_{10} = 1/P_{10}$, are usually considered and therefore, from Eq. (28a)

$$\Theta = \frac{Z_{10}}{K\left[1 - \exp(-h\nu/kT)\right]} \qquad (29)$$

or

$$Z_{10} = K\Theta\left[1 - \exp(-h\nu/kT)\right] \quad . \qquad (30)$$

This is the mean collision lifetime of the first excited state. A similar expression for the mean collision lifetime of the ground state is

$$Z_{01} = - K\Theta\left[1 - \exp(h\nu/kT)\right] \quad . \qquad (31)$$

The collision rate, K, will be considered next. It was found that the most logical approach to use for the hydrocarbons studied here was to proceed from a knowledge of the viscosity of the gases. Amme (1) derived the expression:

$$K\eta = \frac{12.69 \times 10^{7} P}{1 + \frac{BP}{RT}} \qquad (32)$$

where η is the viscosity in centipoise, P the pressure in atmospheres and B the second virial coefficient. The derivation was carried out for a homogeneous maxwellian gas of hard spheres, assuming a weak interaction between spheres and keeping the second virial coefficient. The results from this expression are very good.

For mixtures, a derivation similar to that of Amme (1) is used. The collision rate for the mixture is

$$K = \frac{\bar{\nu}}{L} \qquad (33)$$

where $\bar{\nu}$ is the mean speed of molecules of the mixture and L is their mean free path. The viscosity is

$$\eta = 0.499 \rho \bar{\nu} L \qquad (34)$$

where ρ is the mass density of the mixture. Therefore

$$K\eta = 0.499 \rho \bar{\nu}^2 \quad . \qquad (35)$$

For a mixture, $\rho = (PM_{eff}/RT)$ and $\bar{\nu}^2 = (8RT/\pi M_{eff})$, and so

$$K\eta = 12.88 \times 10^{7} P \quad . \tag{36}$$

This is the same as the expression found by Amme. One can now take account of the Sutherland correction and keep the second virial coefficient to arrive at Eq. (32) for a mixture.

Viscosity data are not available for many of the gases examined, and so some method of calculating η is necessary. Licht and Stechert (17) developed and tested a relation which has proved very satisfactory. Their relation is

$$\eta = 6.30 \times 10^{-6} \left[\frac{M^3 P_c^4}{T_c}\right]^{1/6} \cdot \left[\frac{(T/T_c)^{3/2}}{(T/T_c) + 0.8}\right] \quad . \tag{37}$$

The approximation for the Sutherland constant, $S = 0.8T_c$, used in Eq. (37) is sufficient to yield results accurate to within about five per cent. The results of Eq. (37) have in general been better than first expected.

The viscosity for a mixture is obtained from the viscosities of the pure components by the relation (4):

$$\eta = \frac{\sum_i \chi_i \, \eta_{i\,(M_i)}^{1/2}}{\sum_i \chi_{i\,(M_i)}^{1/2}} \tag{38}$$

where χ_i is the mole fraction present, η_i the viscosity and M_i the molecular weight of the i^{th} component. This

relation has no theoretical background. It was tested (4) and found to predict the viscosities for mixtures to within the precision of the experimental measurements.

In cases where the second virial coefficient is not known, it may be calculated using the Berthelot relation, Eq. (15).

2. Relaxation times for mixtures

It was observed by Amme and Legvold (2) that binary mixtures of gases, which individually show single dispersion, will show single dispersion. One would like to be able to predict this relaxation time.

To look at this problem it is easiest to start with a mixture of a gas, A, which shows dispersion and a gas, B, which does not show dispersion. Let k_{01}^{AA} and k_{10}^{AA} be the number of transitions, $0 \rightarrow 1$ and $1 \rightarrow 0$, per A molecule per second occurring in this mixture due to AA collisions.

It has been established that double collisions are primarily responsible for these energy transfers. Since the double collision rate is proportional to the pressure so also is the number of transitions per molecule per second proportional to the pressure. So if χ is the mole fraction of gas B present then the number of transitions per molecule per second is proportional to $(1 - \chi)$. As discussed in the preceding section, $1/\theta_{AA}$ would be the number of transitions

$1 \longrightarrow 0$ minus the number of transitions $0 \longrightarrow 1$ per molecule per second in pure gas A at one atmosphere pressure where θ_{AA} is the relaxation time for pure gas A. So in the above mixture (total pressure one atmosphere)

$$k_{10}^{AA} - k_{01}^{AA} = \frac{1 - \chi}{\theta_{AA}} \quad . \tag{39}$$

Now define θ_{AB} as the relaxation time of a single A molecule in otherwise pure gas B at one atmosphere. Then in a similar argument the net number of transitions per A molecule per second occurring in the above mixture due to AB collisions is

$$k_{10}^{AB} - k_{01}^{AB} = \frac{\chi}{\theta_{AB}} \quad . \tag{40}$$

If θ_A is the relaxation time of this mixture ($1/\theta_A$ is the net number of transitions per A molecule per second in the mixture due to both AA and AB collisions), one has

$$\frac{1}{\theta_A} = \frac{1 - \chi}{\theta_{AA}} + \frac{\chi}{\theta_{AB}} \quad . \tag{41}$$

The problem is: what happens when gas A and gas B are both dispersive gases?

If one thinks only of the transitions in gas A, Eq. (41) still holds true. Likewise, if only the gas B transitions

are considered one has

$$\frac{1}{\theta_B} = \frac{\chi}{\theta_{BB}} + \frac{1-\chi}{\theta_{BA}} \tag{42}$$

where χ is the mole fraction of gas B present, θ_{BB} is the relaxation time of pure gas B at one atmosphere pressure, θ_{BA} is the relaxation time of a single B molecule in otherwise pure gas A at one atmosphere, and $1/\theta_B$ is the net number of transitions per B molecule per second in the mixture due to both BB and BA collisions.

From the above, $1/\theta_A$ is the net number of transitions per second per molecule of gas A and $1/\theta_B$ is the net number of transitions per second per molecule of gas B. Therefore, the average net number of transitions per second per molecule of the mixture is

$$\frac{1}{\theta} = (1-\chi)\frac{1}{\theta_A} + \chi\frac{1}{\theta_B} \tag{43}$$

where θ is the relaxation time of the mixture and therefore the relaxation time measured experimentally. So we substitute Eq. (41) and Eq. (42) into Eq. (43) and get

$$\frac{1}{\theta} = \frac{(1-\chi)^2}{\theta_{AA}} + \frac{(1-\chi)\chi}{\theta_{AB}} + \frac{\chi^2}{\theta_{BB}} + \frac{\chi(1-\chi)}{\theta_{BA}} . \tag{44}$$

In this equation one can measure everything except θ_{AB} and θ_{BA}. Simultaneous equations for two different mole

fractions, χ, cannot be used to solve for θ_{AB} or θ_{BA} because the coefficients of $1/\theta_{AB}$ and $1/\theta_{BA}$ are the same. So one cannot separate θ_{AB} and θ_{BA} using this method.

It is possible to solve for $(1/\theta_{AB} + 1/\theta_{BA})$ and, vice versa, if $(1/\theta_{AB} + 1/\theta_{BA})$ is known for two given gases one could predict the relaxation time of any percentage mixture of the two by use of Eq. (44).

In the limit where the number of transitions in gas B goes to zero Eq. (44) gives

$$\frac{1}{\theta} = \frac{(1-\chi)^2}{\theta_{AA}} + \frac{(1-\chi)\chi}{\theta_{AB}} \quad . \tag{45}$$

This is the equation which holds for a mixture of a gas A which has dispersion and a gas B which does not. This is not in disagreement with Eq. (41) because $(1/\theta_A)$ is not the same as $(1/\theta)$. $1/\theta_A$ is the number of transitions per second per A molecule in the mixture. $1/\theta$ is the number of transitions per second per molecule of the mixture. θ is the relaxation time calculated from $(\theta = \frac{C_o}{2\pi f_i C_\infty})$ Eq. (10).

C. Prediction of Collision Lifetimes

1. Introduction

Early theoretical treatments of this process were given by Kallmann and London (13), Rice (23), Zener (39, 40),

Jackson and Mott (11), and Landau and Teller (16). Zener (39, 40) used an exponential type potential which is still being used. Landau and Teller (16) discussed the process of energy transfer classically and this helped greatly in the physical understanding of the process.

In more recent years, quantum mechanical treatments have appeared. Of most interest are the works of Schwartz et al. (30), Schwartz and Herzfeld (29), and Tanczos (36). These will be discussed further following the section on the theory of Landau and Teller.

2. The theory of Landau and Teller (16)

It is shown that for the case in which the phenomenon proceeds classically only molecules of high velocity play a role. This can be argued by looking at Ehrenfest's adiabatic principle. This shows that a quantum jump may occur when a system in periodic motion is affected by an external force which changes a relatively large amount during a period of the system. This sort of process is called non-adiabatic.

The transfer of energy from translation to vibration is then dependent on the type of collision. If the period of vibration is small compared to the time of interaction (adiabatic process) there will be no net transfer of energy. In a non-adiabatic process there will be a transfer of

energy. Hence the probability of transfer increases with the ratio of the period of vibration to the interaction time.

This ratio might then be written as

$$\frac{w}{\nu \ell} \tag{46}$$

where w is the relative velocity of approach, ν is the frequency of the vibration, and ℓ is some characteristic length (range of intermolecular forces). The transition probability is assumed to depend on this ratio in an exponential fashion. Then by an integration over a maxwellian distribution of velocities the final expression for the transition probability is found.

This theory is reviewed very clearly by Herzfeld and Litovitz (9) and their result for the transition probability is

$$\frac{1}{Z} = \frac{1}{Z_o} \left(\frac{2\pi}{3}\right)^{1/2} \left(\frac{\epsilon'}{kT}\right)^{1/6} \exp\left[-\frac{3}{2}\left(\frac{\epsilon'}{kT}\right)^{1/3}\right] \tag{47}$$

where $\epsilon' = \tilde{m}(2\pi\nu\ell)^2$, $\tilde{m}$ is the effective mass, and Z is the collision lifetime.

3. Quantum considerations

A quantum mechanical approach for the one-dimensional case was done by Schwartz et al. (30). This is a standard quantum mechanical problem and is carried on to three

dimensions by Schwartz and Herzfeld (29). Tanczos (36) also worked on this and a thorough study of the problem is presented by Herzfeld and Litovitz (9).

The quantum mechanical theory has been applied with fairly good results to simple molecules. Tanczos (36) applied it to the more complex chloromethanes and found good agreement with experiment for two gases but for others the results were off by factors of 8 to 9.

The further complexity of the ethane derivatives leads to great difficulties. It does not appear feasible to apply the quantum theory to the gases studied here.

III. EXPERIMENT

A. Apparatus

1. The interferometer

The variable path interferometer is one of the best instruments for measuring the velocity of ultrasound in gases. Basically it consists of a column limited at one end by a sound source and at the other end by a movable reflector. The reflector is moved away from the source until standing waves are set up (resonance) and then the reflector is moved an additional distance d to another resonance position. The distance between resonance positions will always be equal to some integral number of half wavelengths, n. Therefore, if in the distance d there are n half wavelengths, one can calculate the wavelength from the following relation:

$$\lambda = \frac{2d}{n} \quad . \tag{48}$$

A quartz crystal is the source of sound for this work. The piezoelectric quartz is cut into a disc whose normal is the x-axis and the parallel surfaces are polished optically flat and gold plated. Electrical contact is made to the

surfaces through two of the sliding contacts which hold the crystal in position.

The crystal frequency is determined by the gases to be studied. For the heavy gases considered here it is necessary to reach very high values of f/p (frequency over pressure). Velocity measurements are made as a function of f/p instead of just f because of experimental convenience. To decrease the pressure is to effectively increase the frequency. This is true because the relaxation phenomenon depends upon the number of binary collisions and this is proportional to the pressure.

This suggests that higher frequency crystals would be best. However, present techniques limit the frequencies which can be used with advantage. Crystals with characteristic frequencies up to 2 megacycles per second were studied and tested. Operation of high frequency crystals is very critical and it was concluded that the 400 kilocycle per second crystal gave the best overall results. f/p values up to about 100 megacycles per second per atmosphere are attained by operating at low pressures with the 400 kilocycle crystal. Lambert and Salter (15), with a 4 megacycle crystal, reached values of f/p only up to about 60 megacycles per second per atmosphere.

It is assumed, in theory applied to the interferometer, that one is dealing with plane waves. There are two important points to remember in regard to this.

First, diffraction effects must be minimized. This is accomplished by using a crystal and reflector (in this case both are circular) whose diameters are large compared to the wavelength of the sound wave.

Second, the source should emit waves which are very nearly plane. The crystals used here are about five centimeters in diameter and thus it is expected that there will be areas on the surface which will differ in amplitude and phase of vibration. In order to avoid any undesired radially resonant conditions, for example "Rayleigh modes," from these nuisance vibrations, the chamber diameter is made more than one hundred times greater than the wavelength.

Figure 2 is a cross-section of the interferometer chamber showing the interior details. The reflector rod A extends up to a micrometer screw. The rod is made of Invar steel and is precision machined to pass through an O-ring and a precision bearing K. The bearing K is used to maintain parallelism between the reflector F and the crystal G. The reflector surface is optically flat glass which is gold plated. The crystal has been discussed above. The reflector surface and the top of the crystal are connected by a platimum wire in order to eliminate a troublesome capacitance between the two. B refers to the crystal leads which come from the oscillator. The crystal leads are connected to two of the three sliding contacts J which hold the crystal in position. The temperature gradient is measured by three

Figure 2. The interferometer

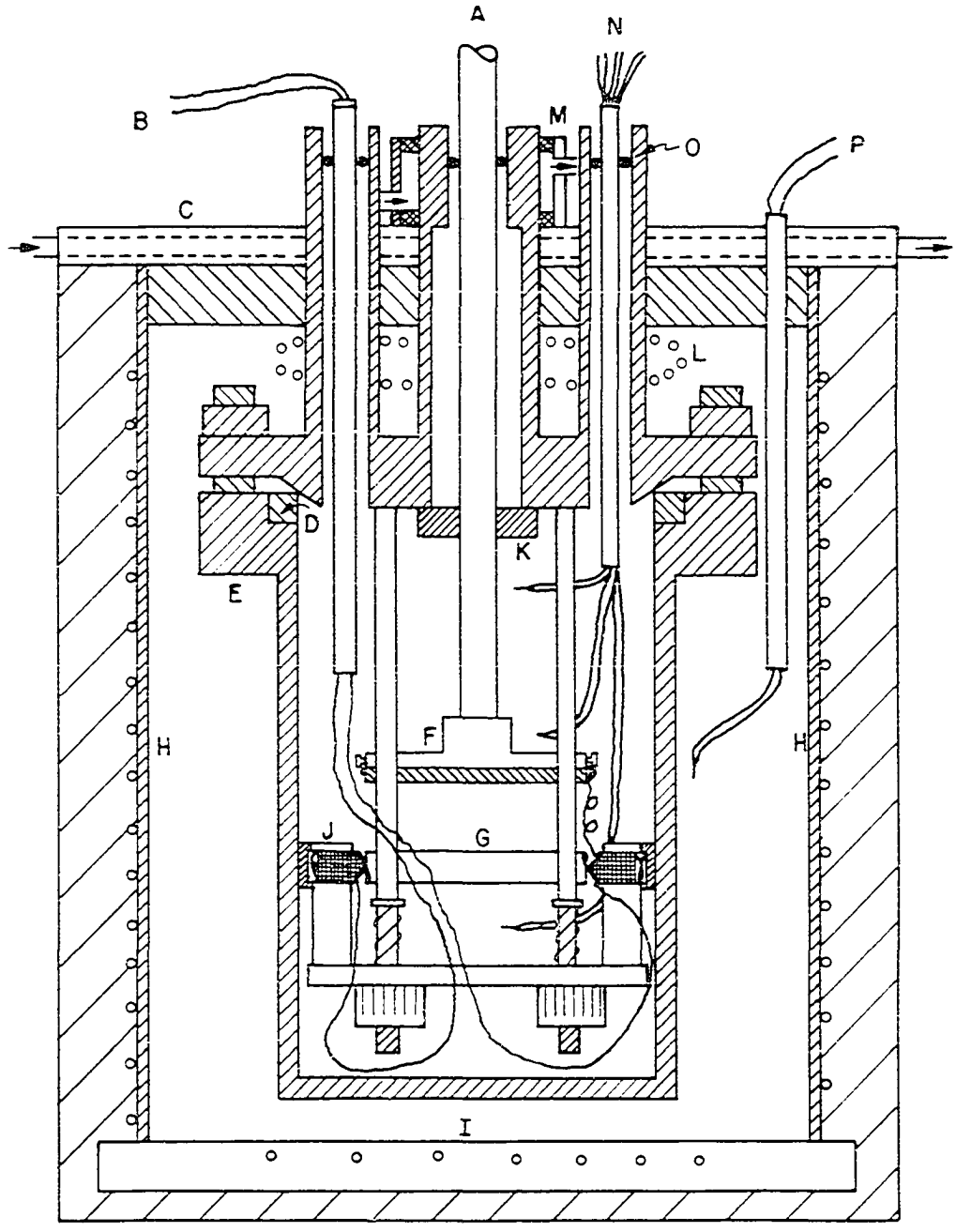
A
N
B
M
O
P
C
L
D
K
E
F
H
H
J
G
I

thermocouples (leads in at N) which are spaced from top to bottom in the chamber. Two of the three leveling screws are shown at the bottom of the system. They are used to align the crystal. The stainless steel chamber E is bolted to the system and vacuum sealed with a copper O-ring D. Neoprene O-rings are used to vacuum seal other leads into the system. Temperature control is aided by the insulating jacket H.

2. Associated equipment

The oscillator used is similar to that used by Rossing (27, 28) and Amme (1) with only slight modifications. The oscillator circuit is shown in Figure 3. The capacitance in the circuit may be varied so as to drive the crystal at its resonance frequency.

The microammeter in the circuit is used to measure a variation in plate current. The plate current varies with the impedance of the crystal and the impedance varies with the reflector position giving sharp peaks at resonance (nodes). To facilitate the determination of node positions the voltage drop across the microammeter is applied to a 0-10 millivolt Brown potentiometer recorder. Therefore the node positions appear as peaks in voltage on the recorder.

The micrometer used to measure the distance between nodes was made by Gaertner and Company. It is 100

Figure 3. The crystal oscillator circuit

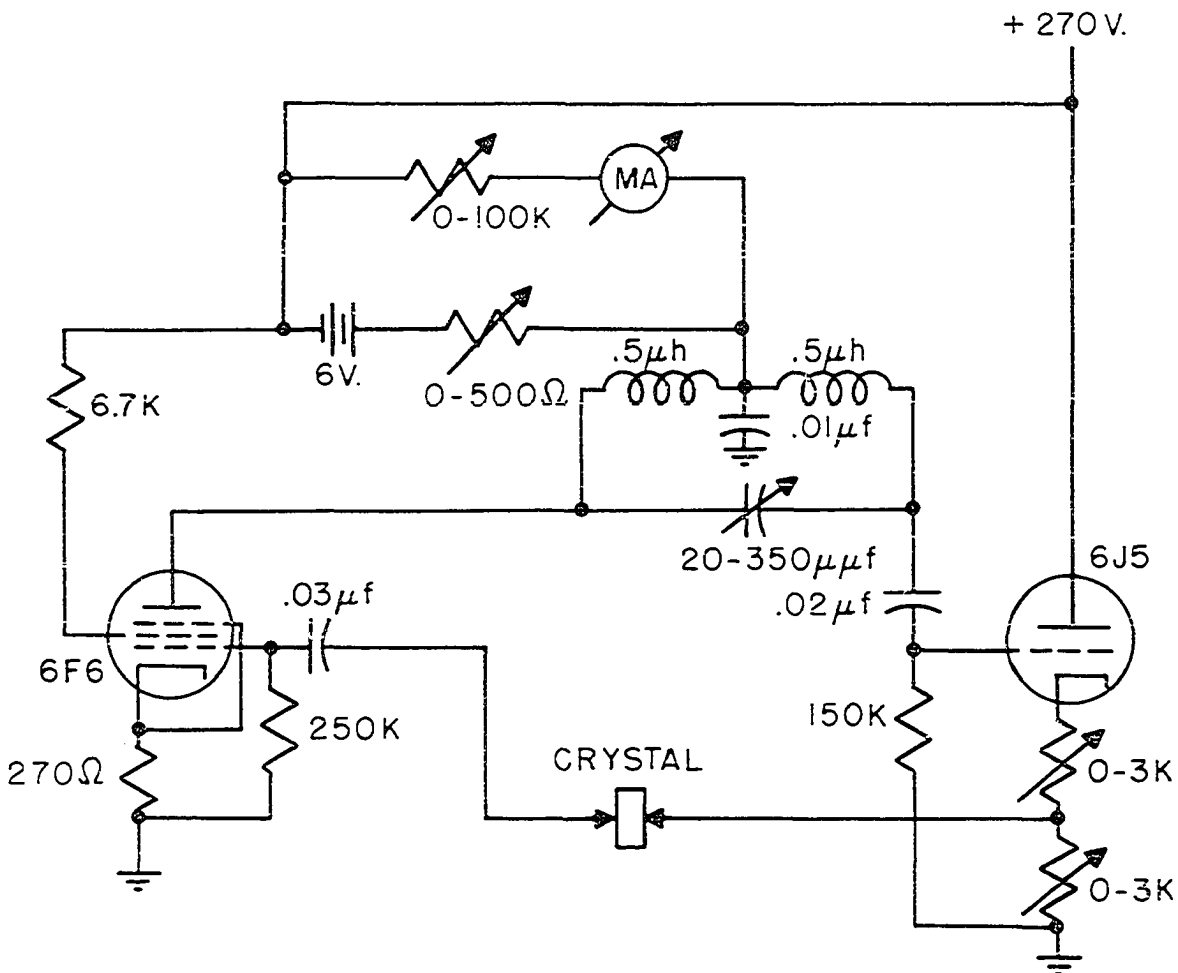
+ 270 V.
MA
0-100K
6V.
0-500Ω
.5μh
.5μh
.01μf
6.7K
20-350μμf
.02μf
6J5
.03μf
6F6
250K
150K
270Ω
CRYSTAL
0-3K
0-3K

millimeters long and can be read to 0.001 millimeter.

The power supply for the oscillator is an electronically regulated power supply of 250 milliamperes capacity. The power supply is fed by a Stabiline voltage regulator.

Additional equipment includes a mercury pressure gauge, a McCleod vacuum gauge, a forepump, and a BC-221 frequency meter.

B. Method

The crystal is properly aligned to parallelism with the reflector. This is done first by eye. Then the peak in voltage as the reflector moves through a node is recorded on a Brown potentiometer recorder. The reflector is moved away from the crystal by a specially geared synchronous motor and a continuous plot of the voltage is the result. One then makes the necessary adjustments for highest peak voltage and for symmetric peaks.

The system is then closed and outgassed enough so that contamination cannot occur during the time a run is being made on a particular gas. A McCleod gauge is used to determine when the system is sufficiently outgassed. The gas to be studied is then admitted to the system.

A run is made by varying the pressure from a high to a low value in such a way as to cover the desired range of f/p values for the gas in question. The gas is put in at the

highest pressure needed and then pumped out to get the values desired for each measurement.

The temperature is observed with the three thermocouples. The thermocouples which were initially calibrated against a standard platinum resistance thermometer are checked periodically by measuring the velocity of sound in argon and comparing results with the National Bureau of Standards results for given temperatures.

Variations in temperature during a given run were usually not more than a few tenths of a degree and standard corrections could be applied to the measured velocities.

The pressure is measured with a mercury U-tube evacuated at one end and open to the system at the other end. The pressure can be read to within about 0.02 of a centimeter or less and so any error here is significant only at very low pressures.

The frequency of the sound wave is determined by the BC-221 frequency meter and is accurate to within about 5 cycles per second for the 400 kilocycle crystal.

The frequency, pressure and temperature are recorded for each value of f/p at which the velocity is measured.

Each velocity recorded is the result of several determinations of the wavelength. The wavelength is determined as follows: The reflector is set near the crystal and then moved slowly away until the voltage on the recorder is near maximum. The voltage and the micrometer reading are both

recorded. Then the reflector is moved on through the peak until the same voltage appears on the recorder. The micrometer reading is again recorded and the average of the two micrometer readings is used as the peak. The procedure is repeated several times at each peak measured. The reflector is then moved further away from the crystal until the peaks are reduced to the minimum readable value or until it is about one centimeter from the first peak. The peak position is again determined as above and the distance d for n peaks is found. This whole procedure is repeated three or four times for each determination of the wavelength. The velocity is then $V = \lambda f$.

At very low pressures absorption is very pronounced and every peak position, starting with the first, is recorded. At the lowest pressures used only three to five peak positions could be determined.

The mixtures were made by first adding one gas and reading the pressure then adding the second gas and noting the increase in pressure. According to the law of partial pressures this would give one the percentage of each gas present if they were ideal gases. The standard correction for the difference in molecular density of the two gases is applied to the ideal percentages to bring one nearer the real case.

It is necessary to let mixtures set for several hours to assure that they are thoroughly mixed. The procedure is

then the same as for a single gas.

Since the gases used were stored as liquids under high pressure, the liquids were drawn from inverted cylinders to eliminate contamination due to noncondensable gases over the liquids.

IV. RESULTS AND DISCUSSION

A. Experimental

An examination of the ethane derivatives for sound dispersion was the first step in this investigation. C_2H_6, $CClF_2CClF_2$, CH_3CH_2Cl, CH_3CHF_2, and CH_3CClF_2 were examined at room temperature. Ethane shows double dispersion and the other gases show single dispersion (Figures 4 through 8).

The double dispersion is a very interesting case because the lowest mode of vibration is a hindered mode of rotation. This is true also for the four ethane derivatives. However, there is one very evident difference and that is in the frequency gap between the lowest mode of vibration (hindered rotation) and the next lowest mode of vibration. For ethane the frequency gap is about 530 cm^{-1} while for the three ethane derivatives, for which the fundamental modes of vibration are known, the frequency gap is always less than 150 cm^{-1}. (The fundamental modes of vibration are listed in Table 1.)

A look at the fundamental modes of vibration of ethylene shows that a mixture of ethylene and ethane would have a frequency gap just about the same size as that for pure ethane. Such mixtures should show double dispersion. These velocity curves along with that for pure ethylene are shown in Figures 9 through 12.

Table 1. Frequency of the fundamental modes of vibration in cm^{-1}

C_2H_6(33)	CH_3CH_2Cl(5)	CH_3CHF_2(35)	CH_3CClF_2(34)	C_2H_4(3)	$CClF_2CClF_2$
290*	236*	236*	238*	810.3	(not known)
821.5-2	336	383	305	943	
993	676	470	334	949.2	
1190-2	785	571	435	1027*	
1375	972-2	868	526	1236	
1379.1	1080	930	543	1342.4	
1460-2	1245	1129	683	1443.5	
1472.2-2	1287	1143	904	1623.3	
2899.2	1383	1169	967	2989.5	
2954	1452-3	1360	1107	3019.3	
2963-2	2878	1372	1202	3105.3	
2995.5-2	2890	1414	1230	3272.3	
	2940	1460-2	1395		
	2983	2963	1447-2		
	3012	2979	2965		
		3001	3035-2		
		3017			

* mode of hindered rotation.

- denotes degeneracy of mode.

Figure 4. Velocity dispersion in CH_3CH_2Cl at 296.5° K

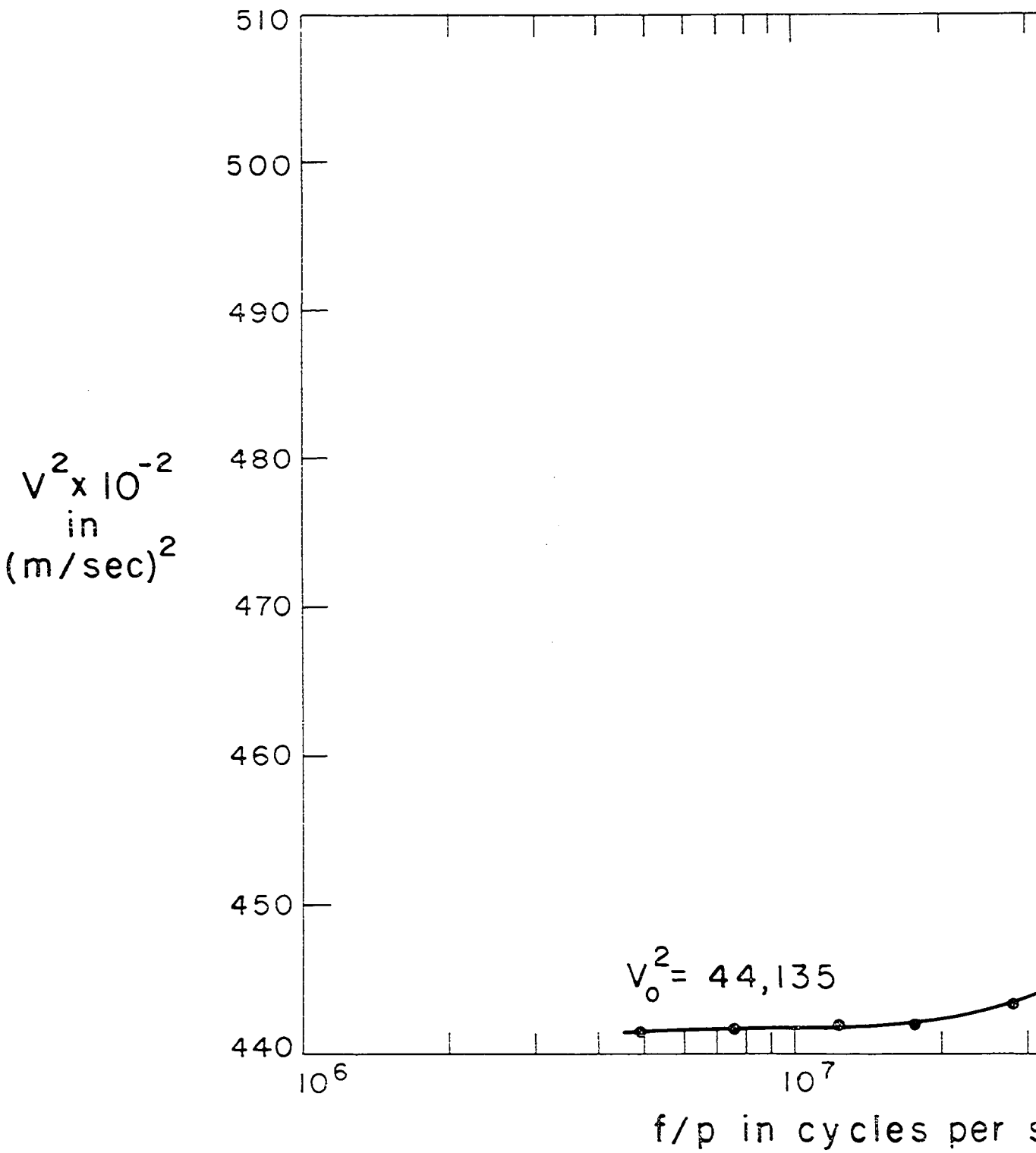
510
500
490
480
470
460
450
440
$V^2 \times 10^{-2}$ in $(m/sec)^2$
$V_o^2 = 44,135$
10^6
10^7
f/p in cycles per s

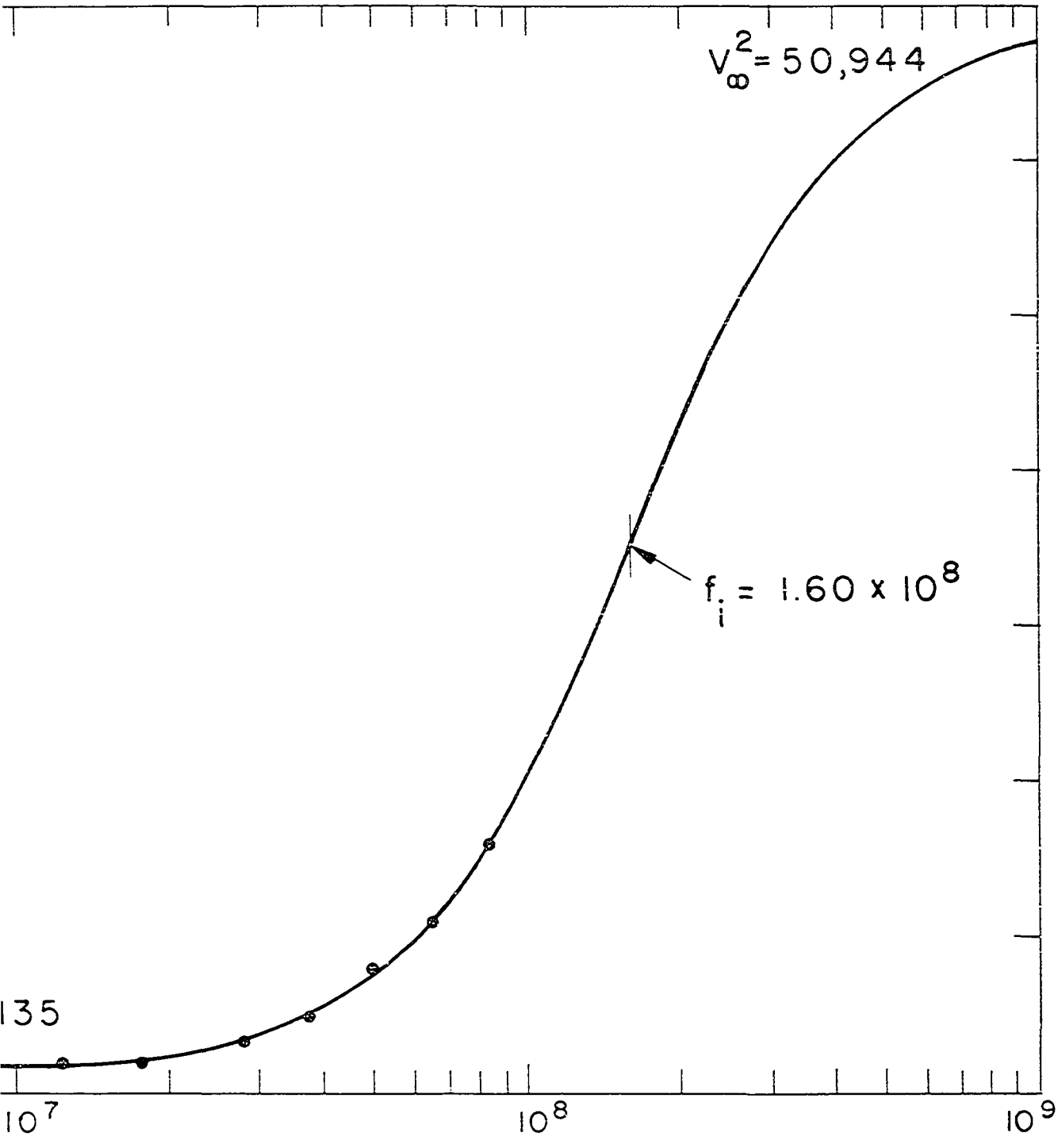
$V_\infty^2 = 50{,}944$
$f_i = 1.60 \times 10^8$
135
10^7
10^8
10^9
cycles per second - atmosphere

Figure 5. Velocity dispersion in CH_3CHF_2 at 296.1° K

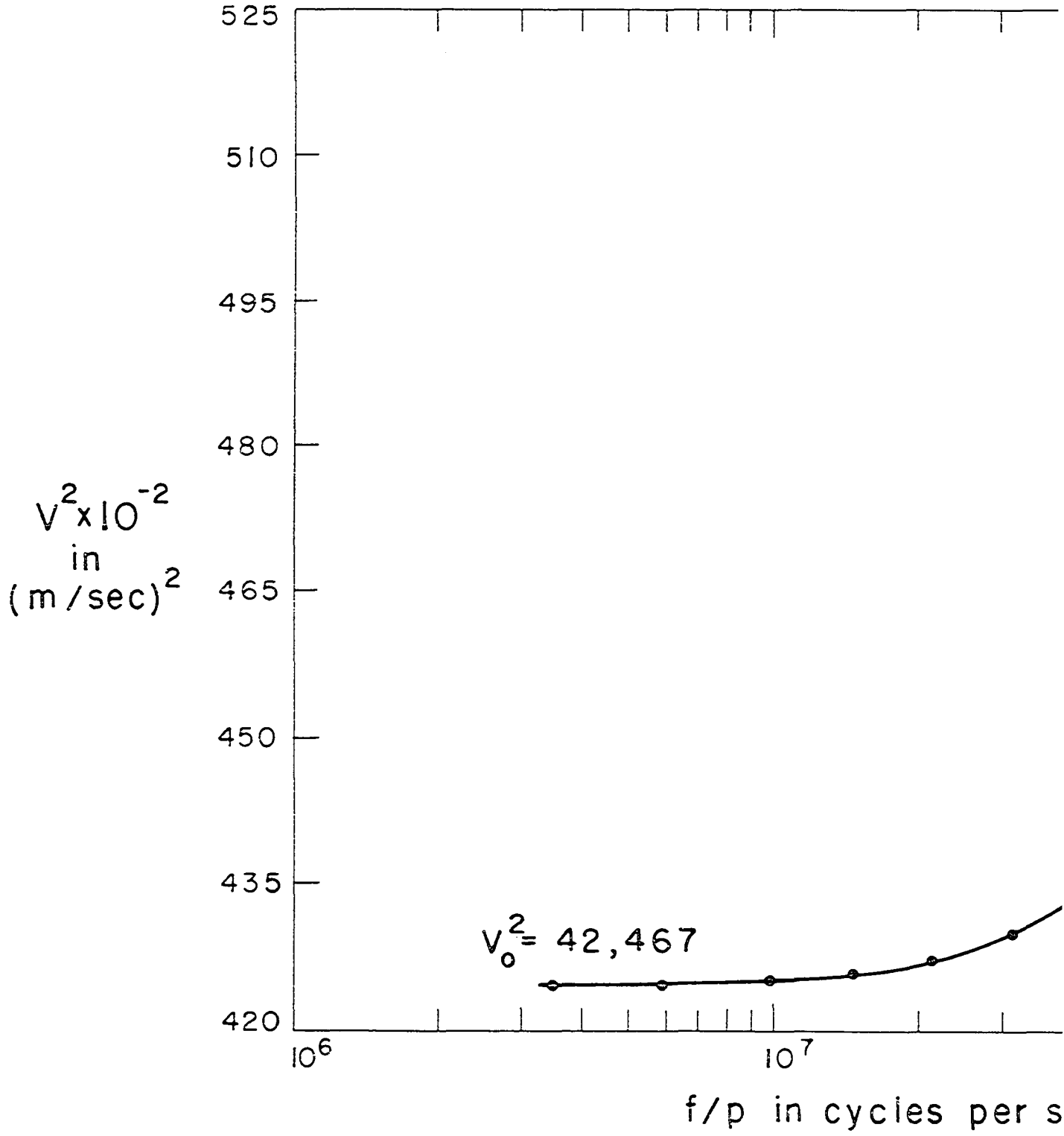
525
510
495
480
465
450
435
420
$V^2 \times 10^{-2}$ in $(m/sec)^2$
$V_o^2 = 42,467$
10^6
10^7
f/p in cycles per s

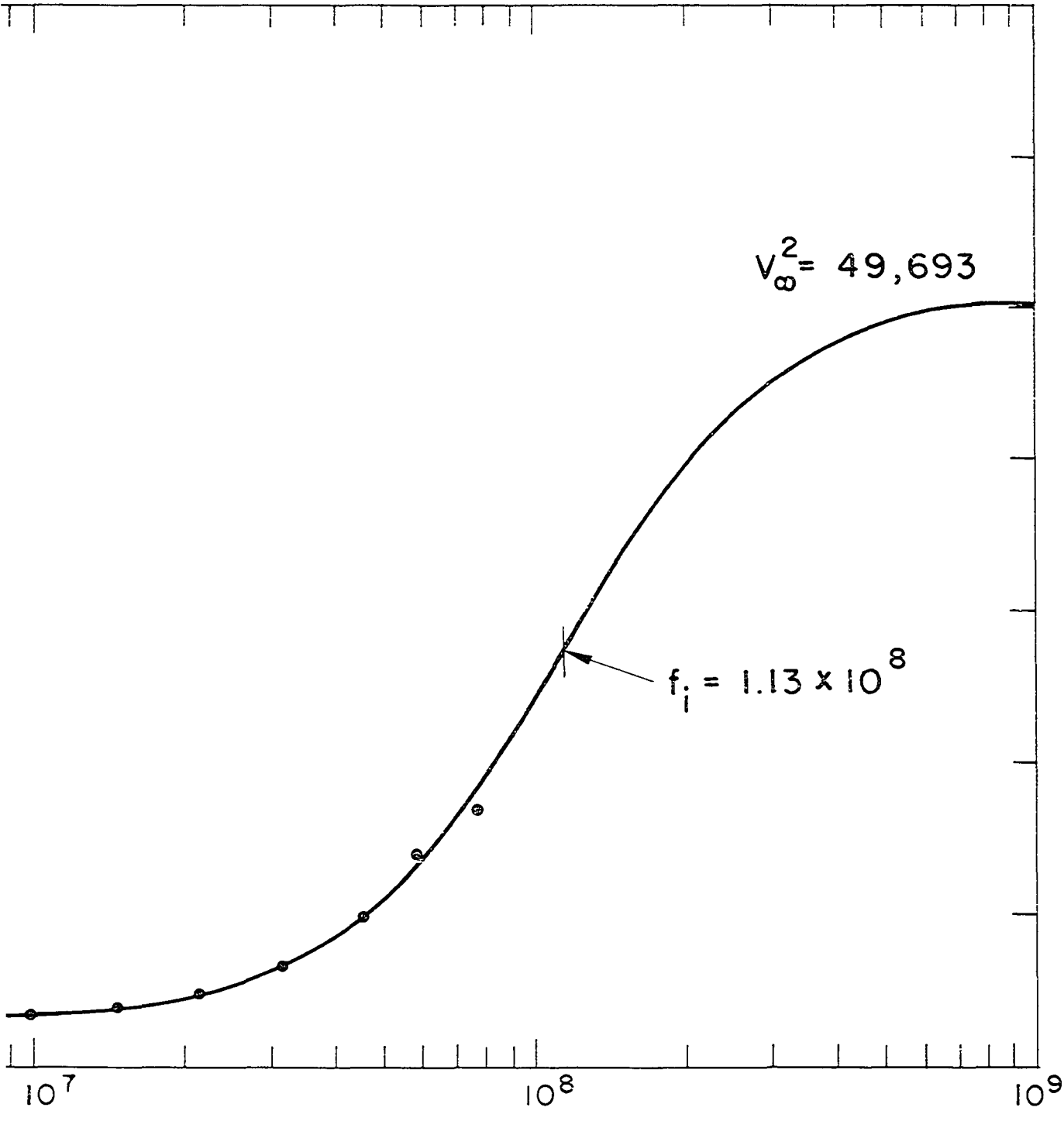
$V_\infty^2 = 49{,}693$
$f_i = 1.13 \times 10^8$
10^7
10^8
10^9
in cycles per second-atmosphere

Figure 6. Velocity dispersion in $CClF_2CClF_2$ at 296.88° K

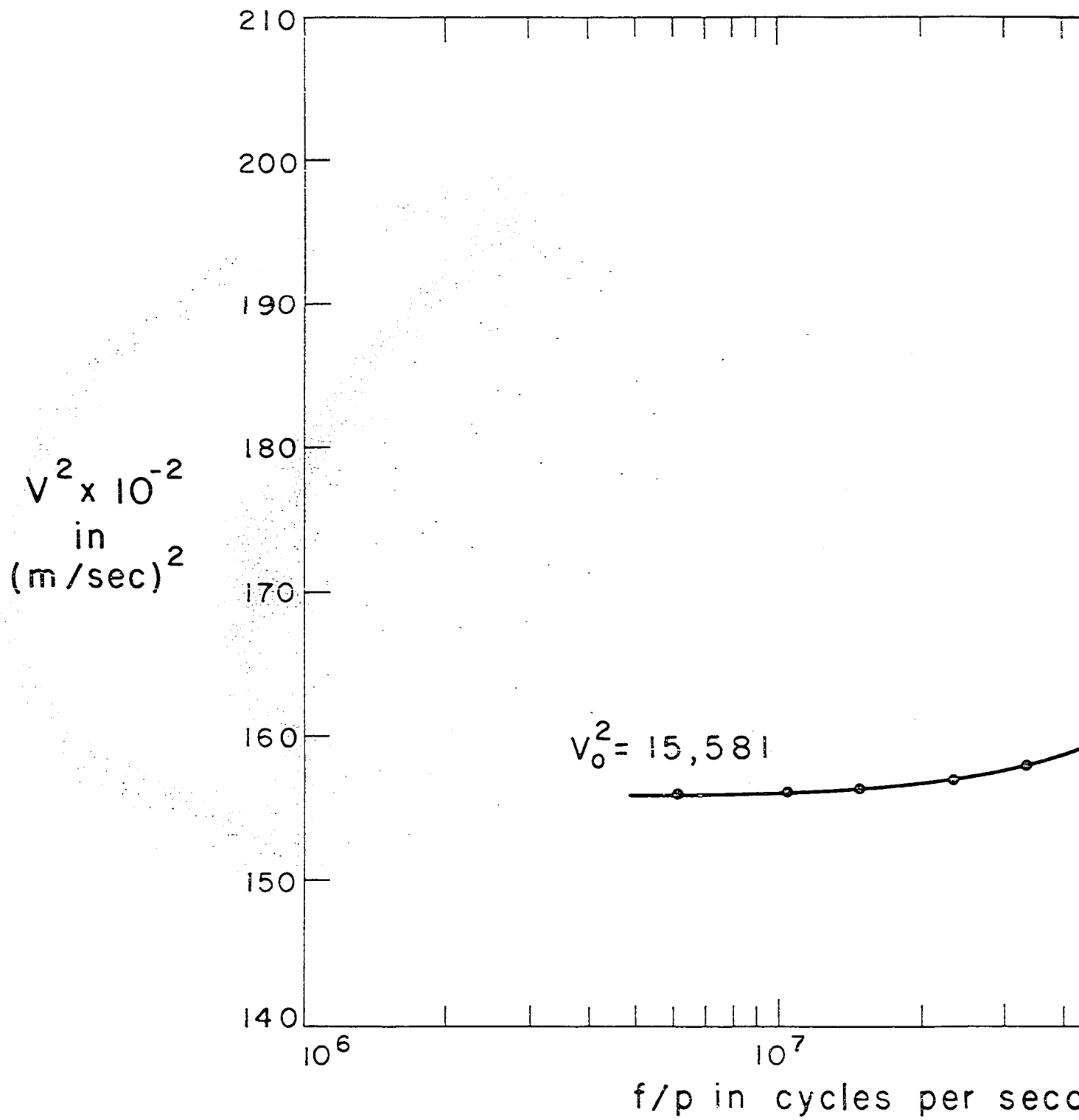
210
200
190
180
170
160
150
140
$V^2 \times 10^{-2}$
in
$(m/sec)^2$
$V_o^2 = 15,581$
10^6
10^7
f/p in cycles per secc

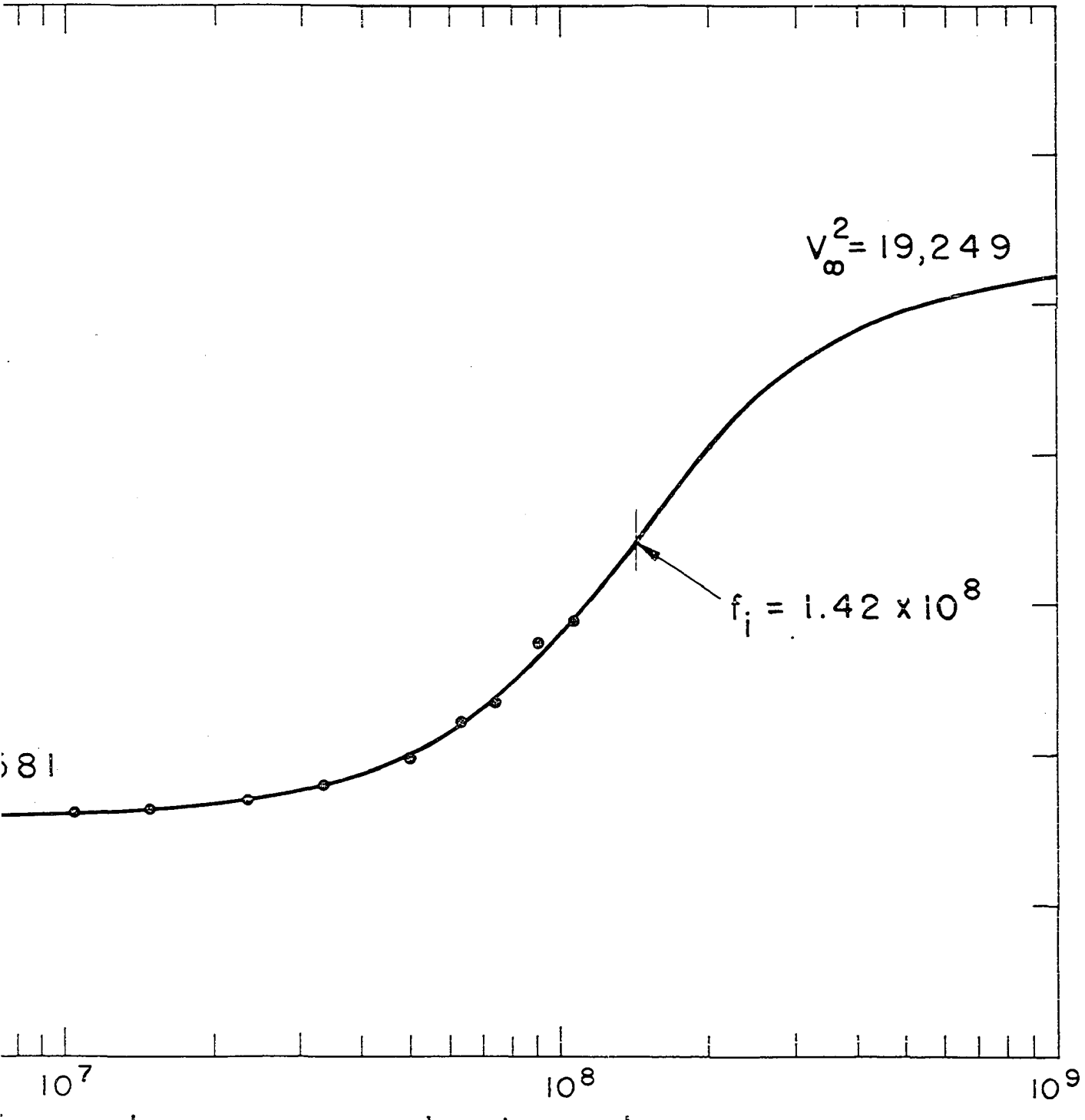
$V_\infty^2 = 19{,}249$
$f_i = 1.42 \times 10^8$
581
10^7
10^8
10^9
in cycles per second - atmosphere

Figure 7. Velocity dispersion in CH_3CClF_2 at 295.5° K

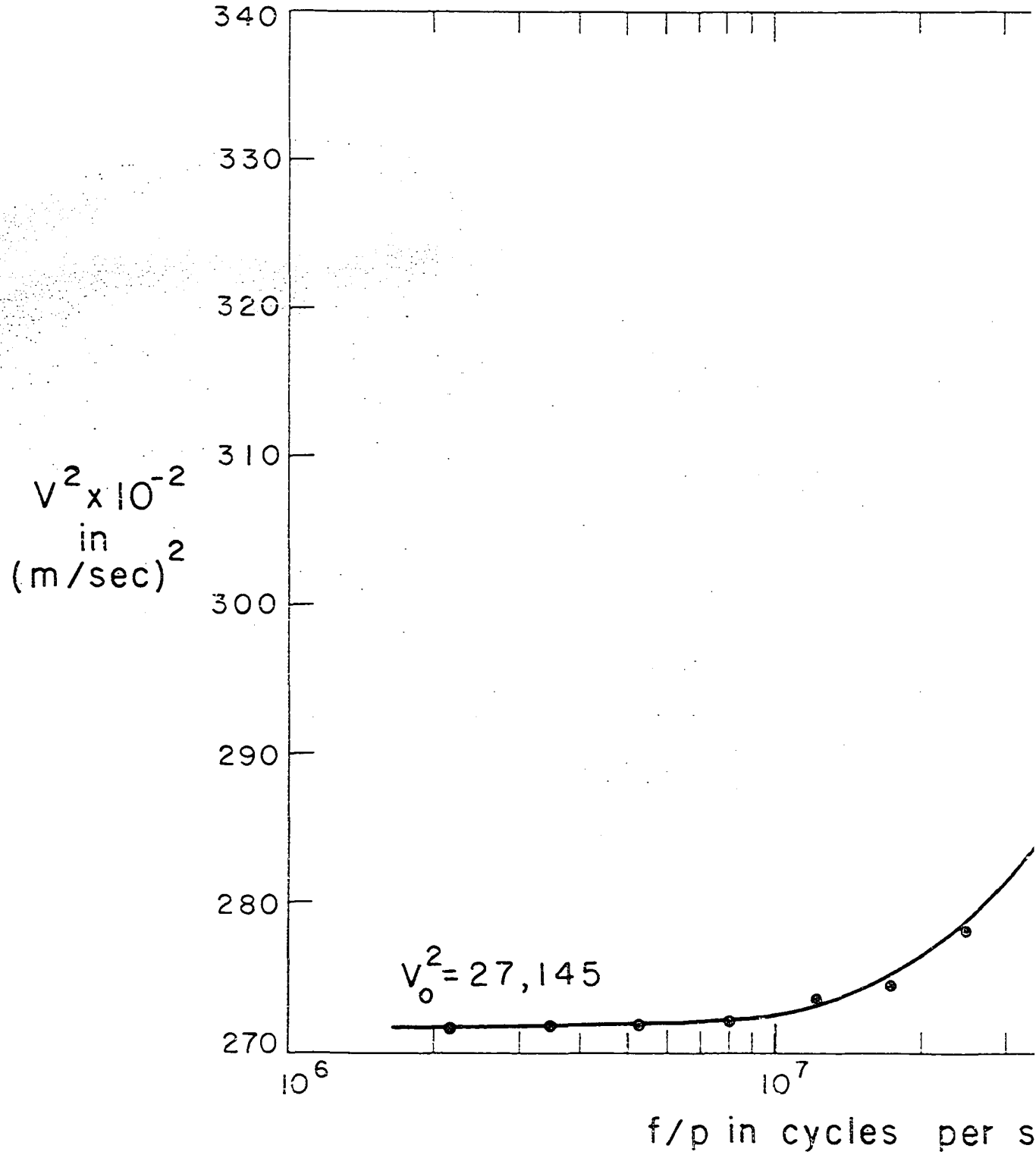
340
330
320
310
300
290
280
270
$V^2 \times 10^{-2}$ in $(m/sec)^2$
$V_o^2 = 27,145$
10^6
10^7
f/p in cycles per s

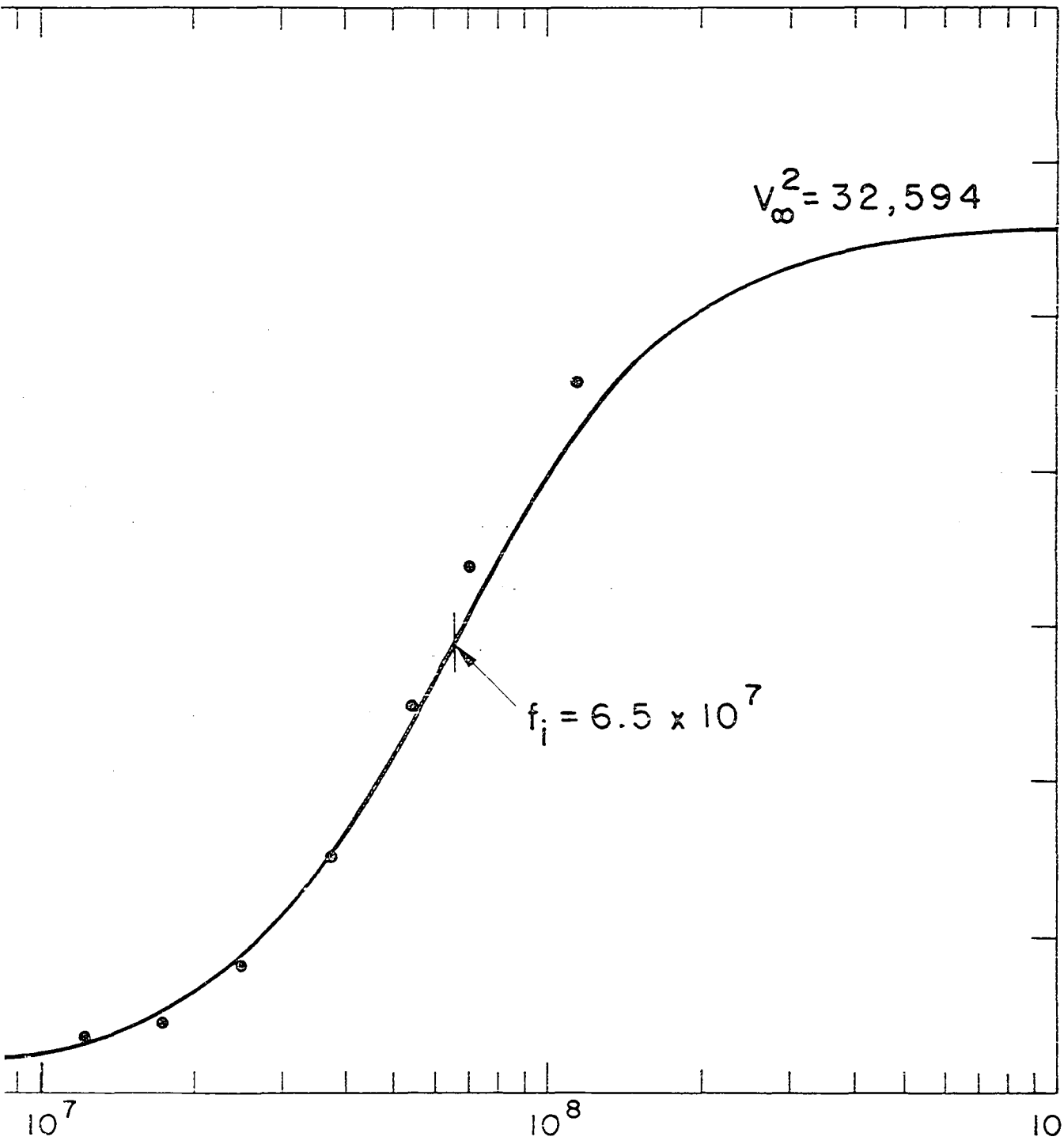

n cycles per second - atmosphere

Figure 8. Velocity dispersion in C_2H_6 at 296.6° K

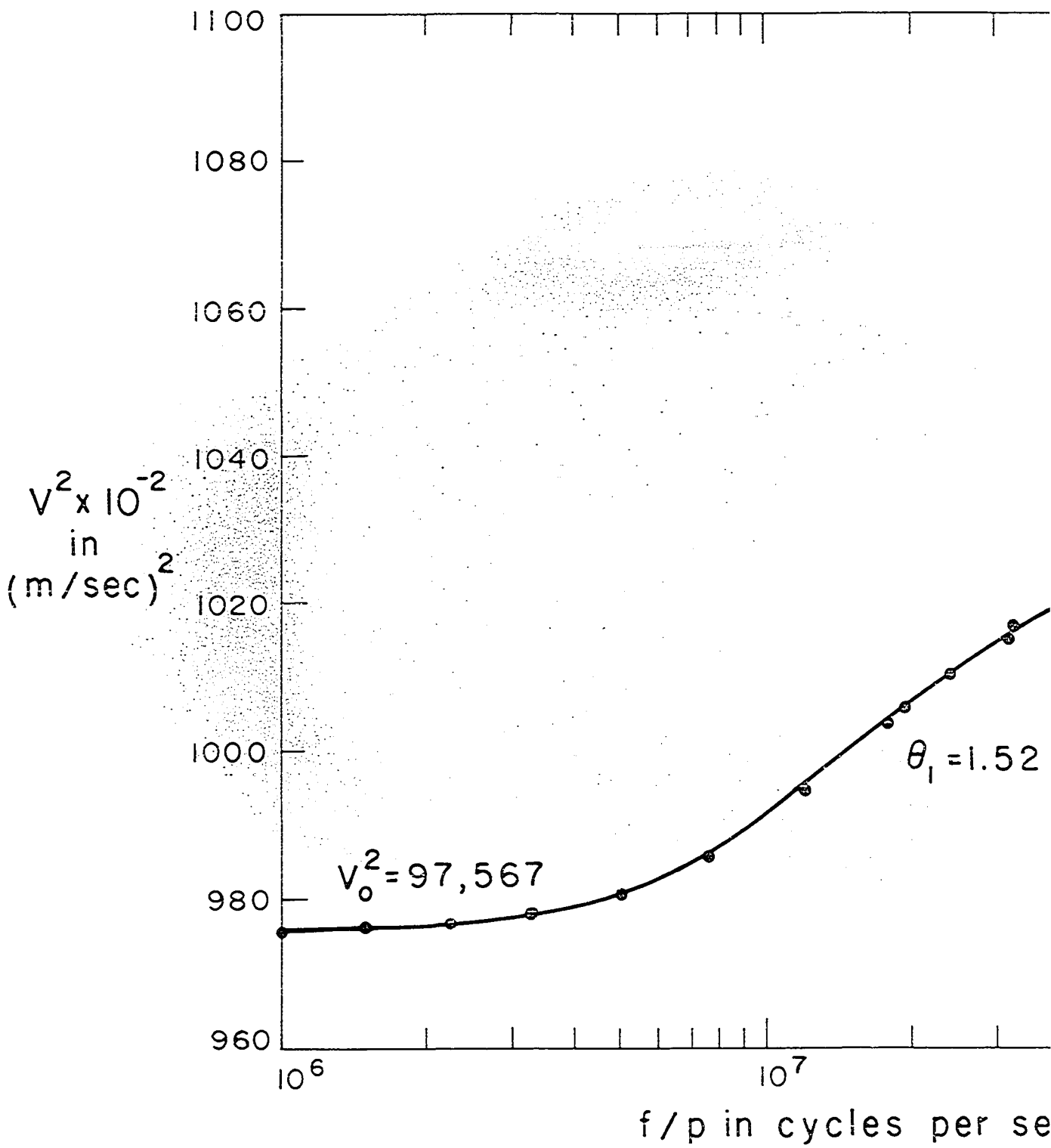
1100
1080
1060
1040
1020
1000
980
960
$V^2 \times 10^{-2}$ in $(m/sec)^2$
$V_o^2 = 97,567$
$\theta_1 = 1.52$
10^6
10^7
f/p in cycles per se

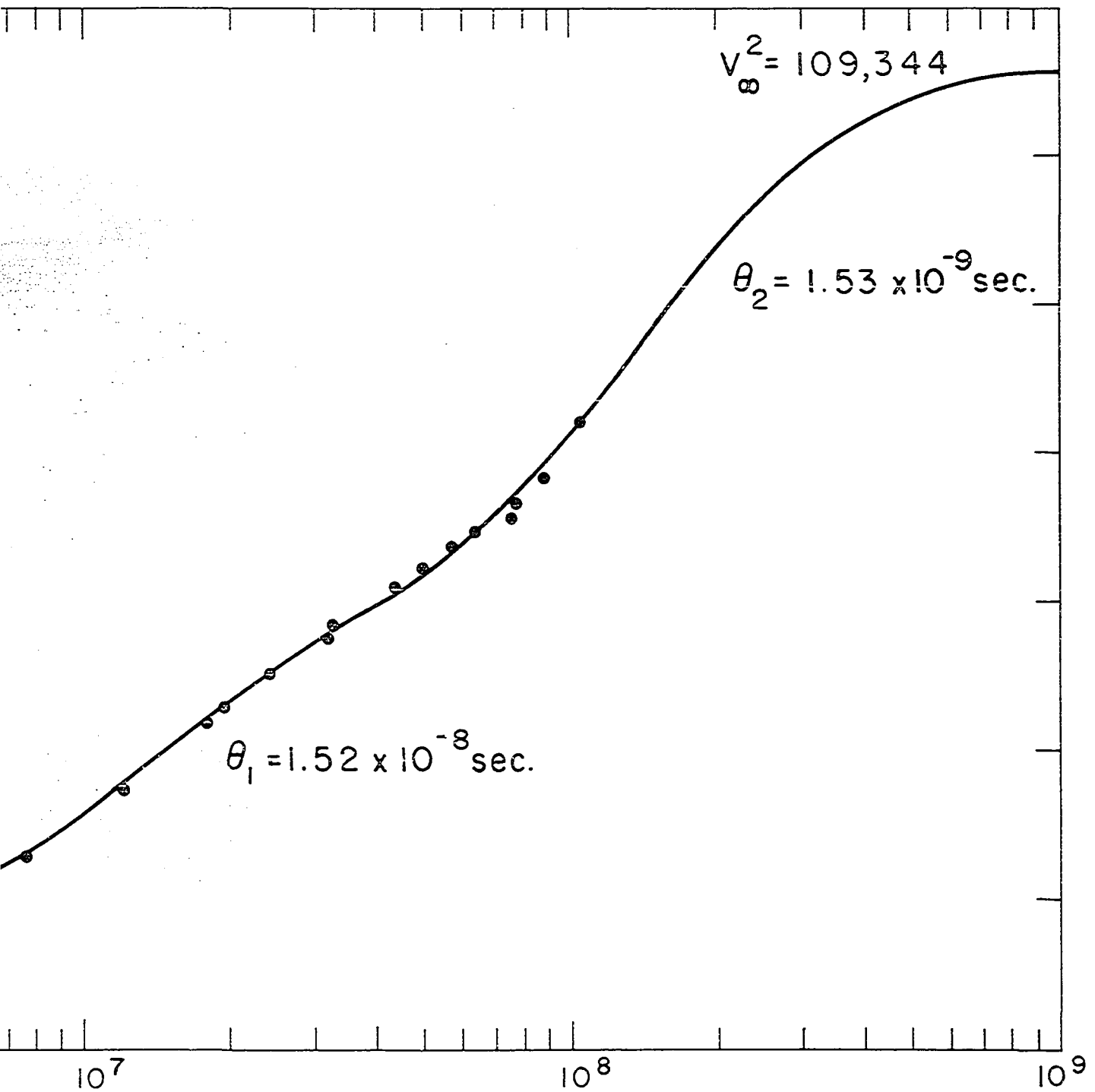

p in cycles per second - atmosphere

Figure 9. Velocity dispersion in a 75.1% C_2H_6 - 24.9% C_2H_4 mixture at 296.6° K

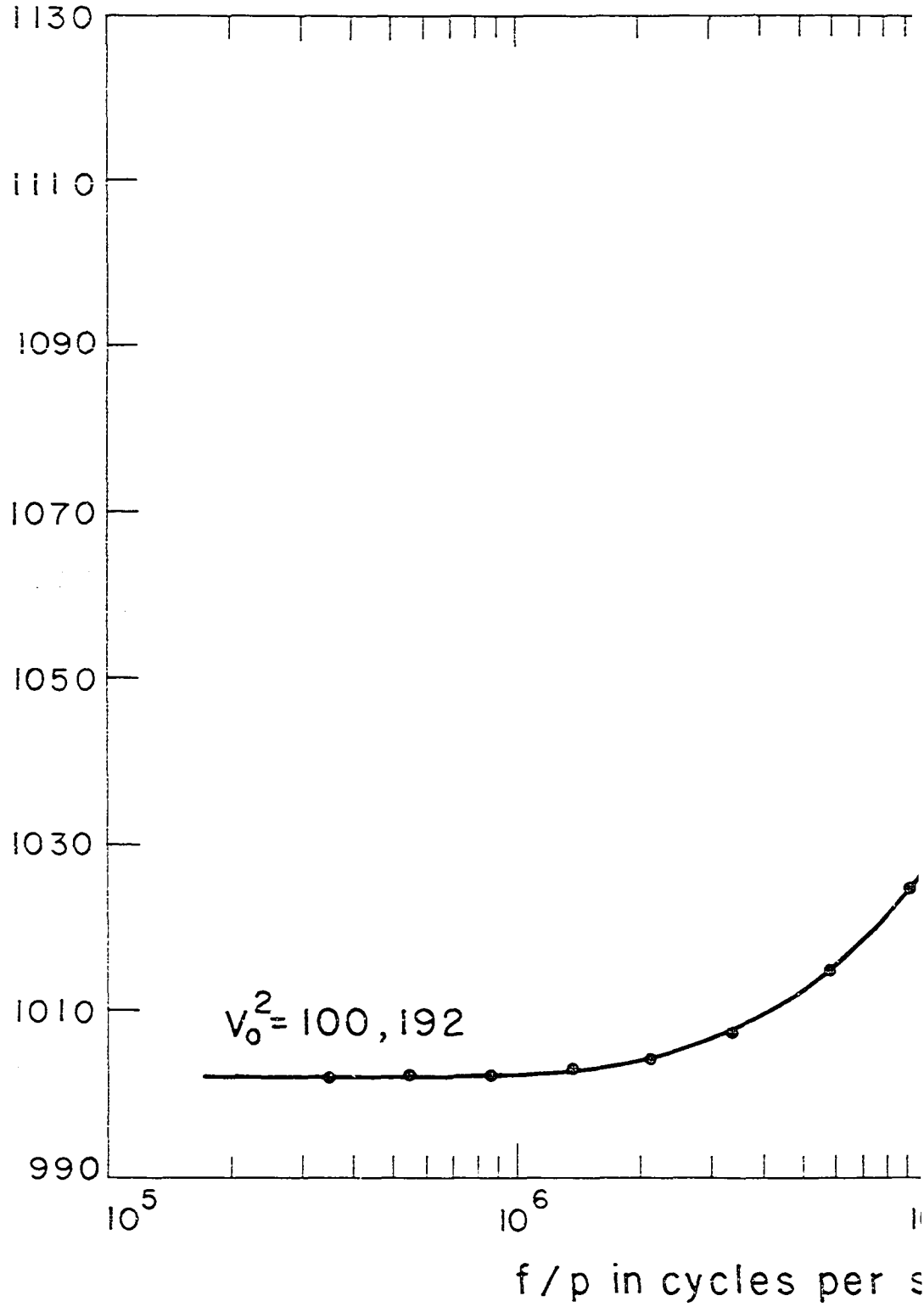
1130
1110
1090
1070
1050
1030
1010
990
$V^2 \times 10^{-2}$
in
$(m/sec)^2$
$V_0^2 = 100,192$
10^5
10^6
f/p in cycles per s

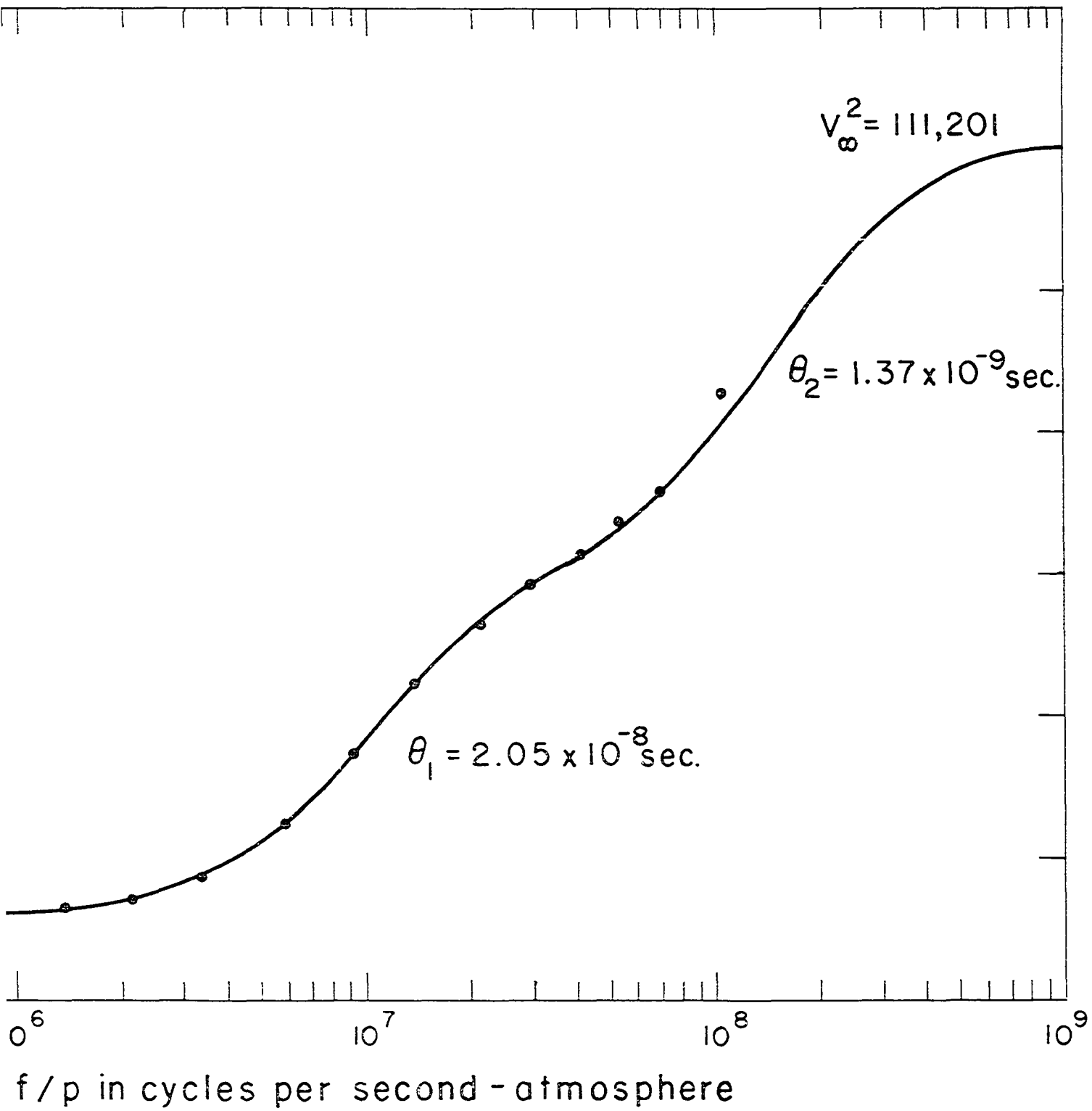
$V_\infty^2 = 111{,}201$
$\theta_2 = 1.37 \times 10^{-9}$ sec.
$\theta_1 = 2.05 \times 10^{-8}$ sec.
10^6
10^7
10^8
10^9
f/p in cycles per second - atmosphere

Figure 10. Velocity dispersion in a 49.5% C_2H_6 - 50.5% C_2H_4 mixture at 296.6° K

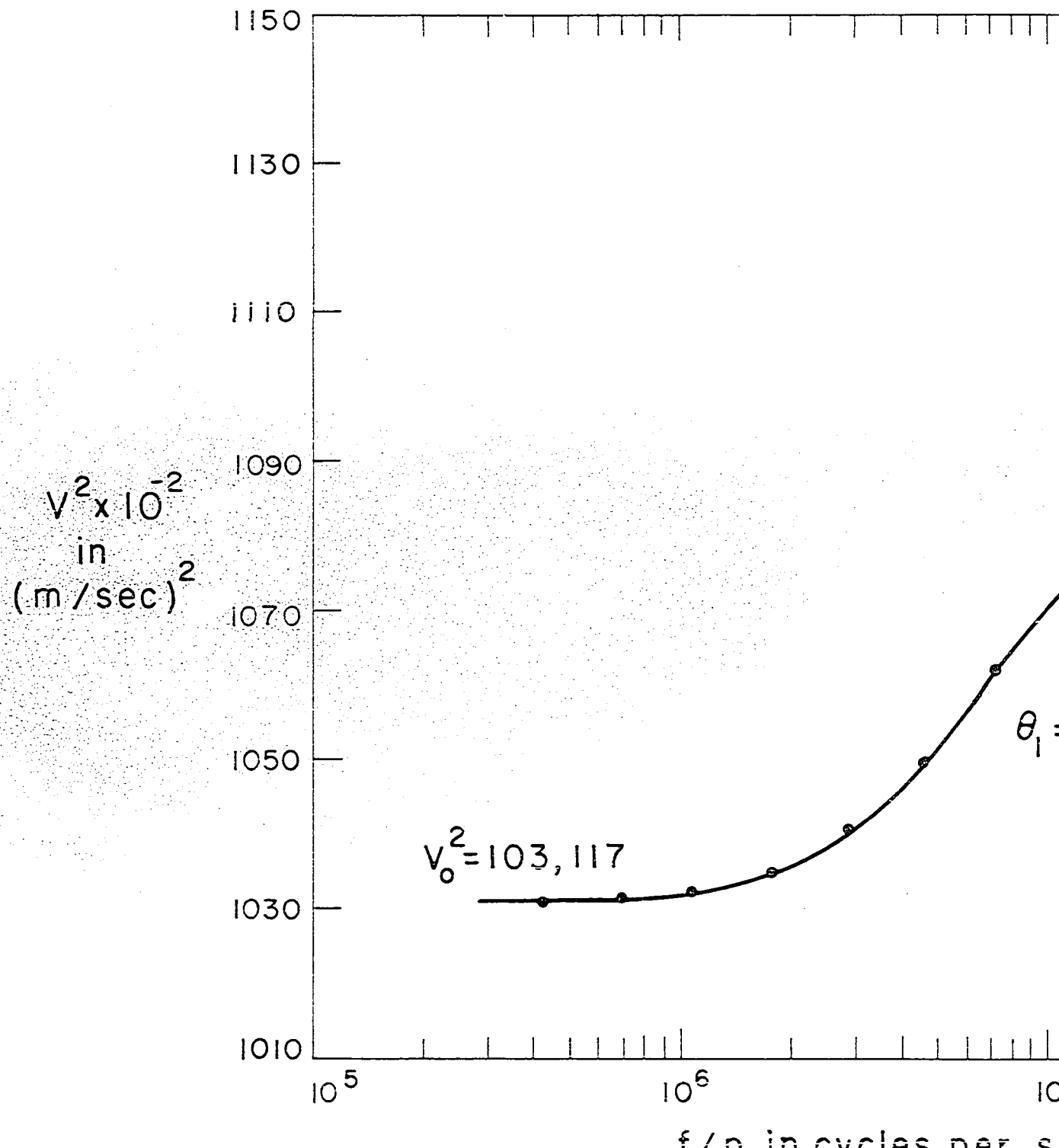
1150
1130
1110
1090
1070
1050
1030
1010
$V^2 \times 10^{-2}$
in
$(m/sec)^2$
$V_o^2 = 103,117$
θ_1 =
10^5
10^6
f/p in cycles per s

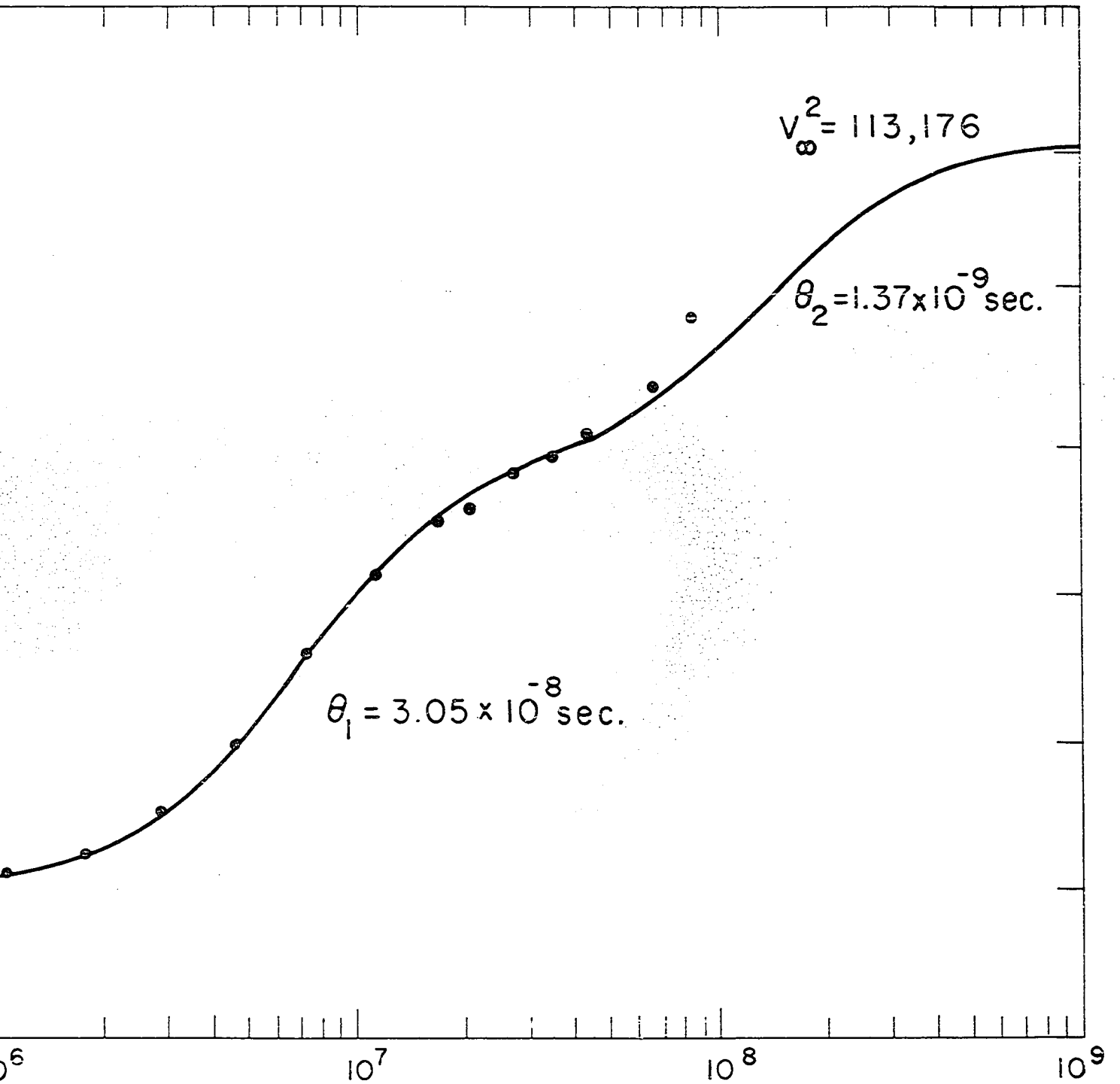

f/p in cycles per second - atmosphere

Figure 11. Velocity dispersion in a 25.1% C_2H_6 - 74.9% C_2H_4 mixture at 296.6° K

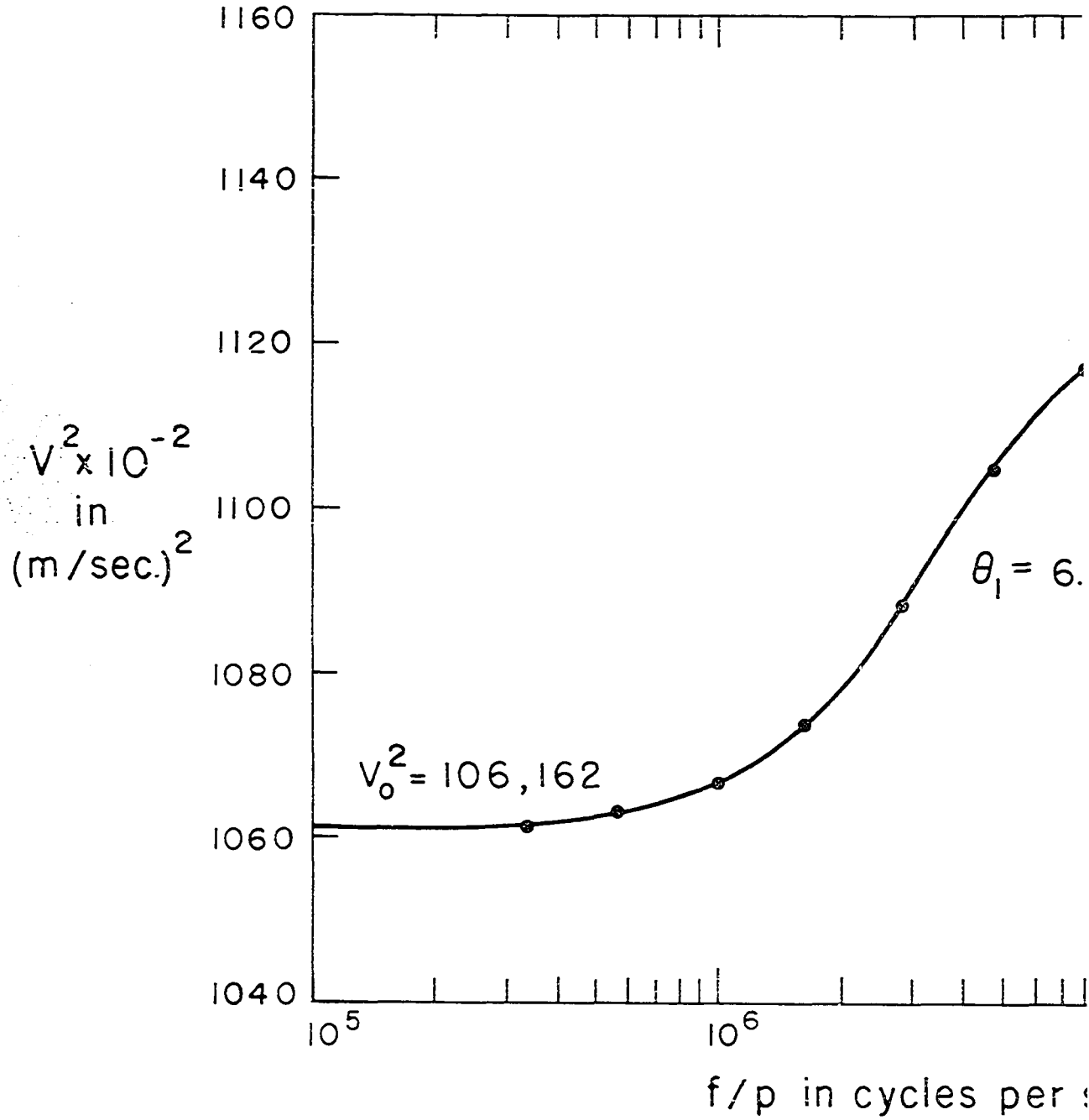
1160
1140
1120
1100
1080
1060
1040
$V^2 \times 10^{-2}$
in
$(m/sec.)^2$
$V_o^2 = 106,162$
$\theta_1 = 6.$
10^5
10^6
f/p in cycles per

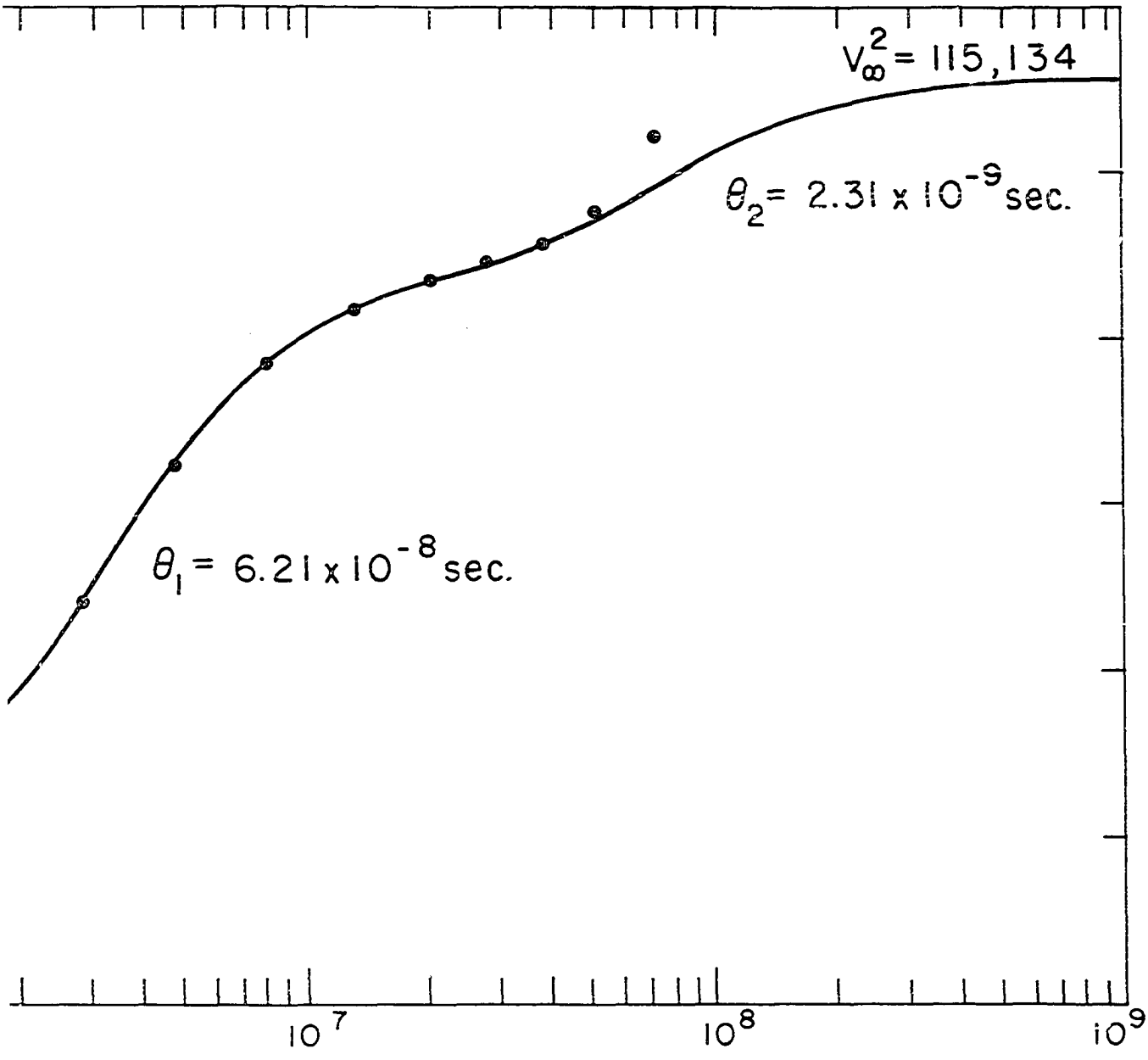

cycles per second - atmosphere

Figure 12. Velocity dispersion in C_2H_4 at 296.6° K

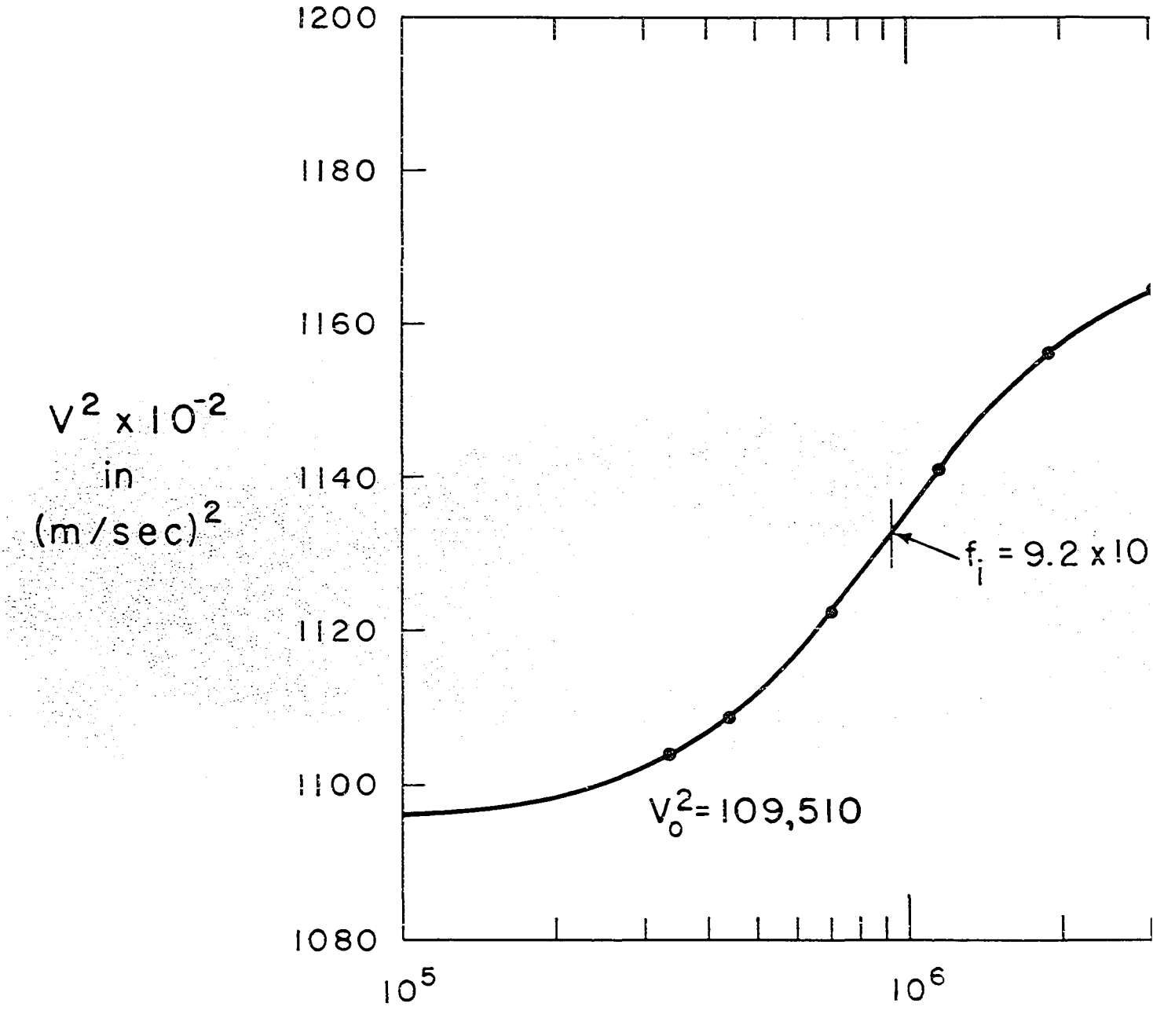
1200
1180
1160
1140
1120
1100
1080
$V^2 \times 10^{-2}$
in
$(m/sec)^2$
$f_i = 9.2 \times 10$
$V_o^2 = 109,510$
10^5
10^6
f/p in cycles per sec

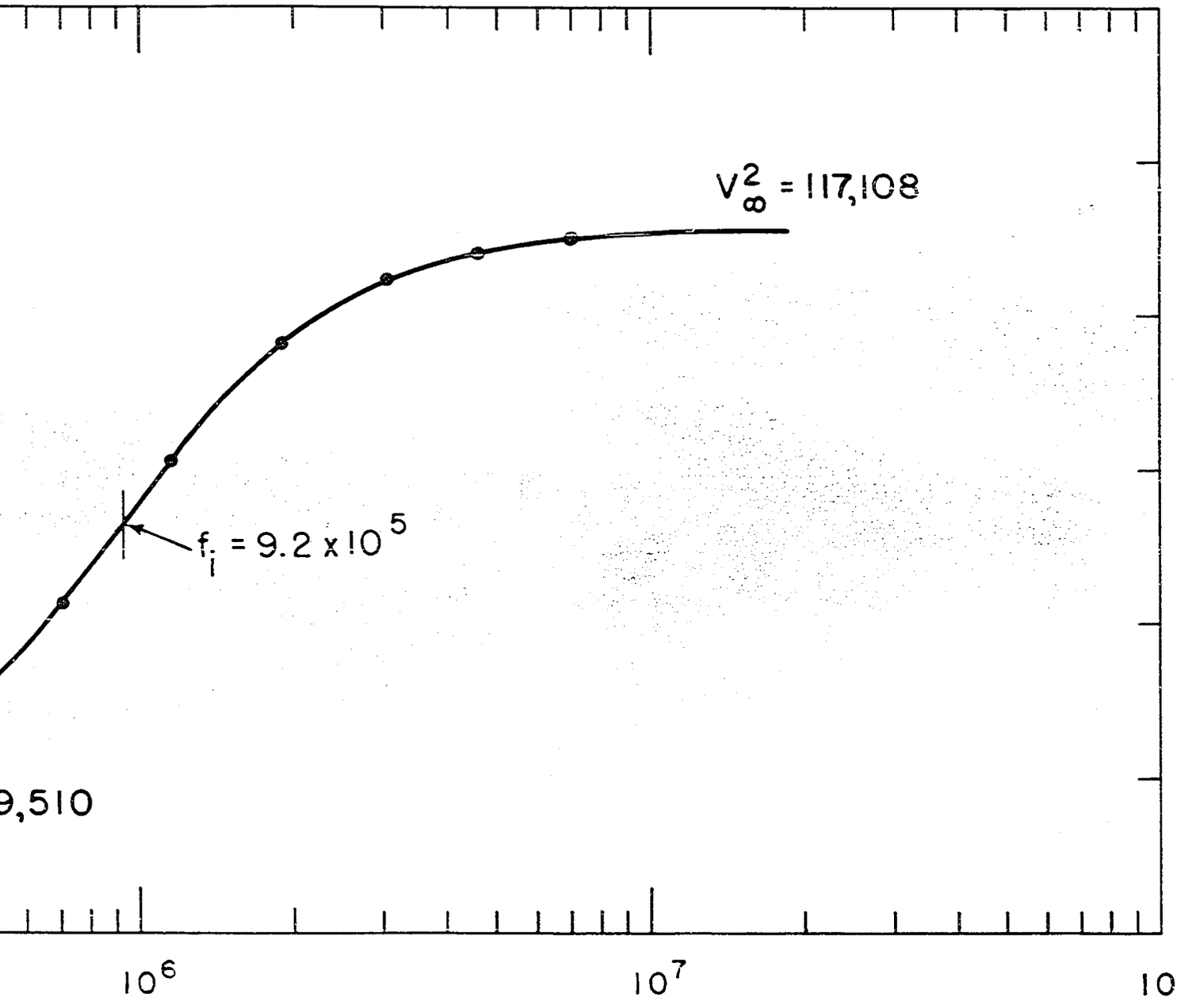
V_∞^2 = 117,108
f_i = 9.2 x 10^5
9,510
10^6
10^7
10^8
cycles per second-atmosphere

The double dispersion curves make clear that the exchange mode for the ethane derivatives is the lowest mode of "regular" vibration. The ethane-ethylene curves show that the first step in the dispersion is due to a combination of the pure ethylene vibrational specific heat and the specific heat of the "regular" vibrations (not hindered rotation) of pure ethane. The second step is always due to the specific heat of the hindered rotational mode in ethane. Therefore one notes that the heat capacity of a "regular" vibration will tend to lag at a lower frequency sound wave than the mode of hindered rotation even though the "regular" vibration has a much higher frequency. This tells us that in calculating the collision lifetimes for the four ethane derivatives, which show single dispersion, one must use as the exchange mode the lowest "regular" vibrational mode not the lower mode of hindered rotation.

Table 2 lists information and results for the four ethane derivatives which show single dispersion. The gas purities listed are those reported by the Matheson Company from whom the gases were obtained. ν_e and C_e are values for the lowest "regular" mode of vibration; η is calculated using the relation of Licht and Stechert (17), Eq. (37); and C_{vib} is found from the experimental C_o by Eq. (20). Z_{10} is then the collision lifetime for de-excitation of the exchange mode.

Table 2. Purity, T, M, ν_e, η, $1 + \frac{B}{RT}$, f_i, θ, C_e, C_{vib}, θ_e, K, and Z_{10} for the four ethane derivatives

Gas	CH_3CH_2Cl	CH_3CHF_2	$CClF_2CClF_2$	CH_3CClF_2
purity	99.99%	98%	95%	98%
T° K	296.50	296.10	296.88	295.50
M	64.519	66.049	170.90	100.503
$\nu_e (cm^{-1})$	336	383	-	305
$\eta \times 10^2$ cp	0.898	1.104	1.167	1.098
$1 - \frac{B}{RT}$	0.9706	0.9826	0.9662	0.9744
$f_i \times 10^{-8}$	1.60	1.13	1.42	0.65
$\theta \times 10^9$	2.14	3.37	4.73	7.39
C_e	1.60	1.50	~1.60	1.66
C_{vib}	6.85	8.29	19.18	12.03
$\theta_e \times 10^{10}$	5.0	6.1	~7.9	10.2
$K \times 10^{-10}$	1.46	1.17	1.12	1.19
Z_{10}	5.9	6.0	~7.0	9.4

~ Indicates that the values are based on an estimate.

The % error is determined in the usual manner. An ideal velocity curve is plotted on a separate sheet and then shifted along the abscissa over the data until the best fit is obtained. Then moving the curve to the left and right one finds a range in which the curve might be considered to fit.

This then sets the limits on the inflection frequency, f_i. Even though the data do not go very far into the dispersive region for some of the ethane derivatives the percentage error in locating the inflection frequency may be considered to be always less than 10%. All sources of error are then incorporated into this one technique for a general determination of error.

All of the collision lifetimes are less than ten, therefore, the number of transitions per second is very large because of the high collision rate, K. This restores the system to equilibrium, very rapidly making it necessary to reach very high frequency sound waves before a heat capacity lag is observed.

Table 3 lists the information and results for ethane, ethylene and their mixtures. Double dispersion is observed whenever ethane is present. The purity of the ethane and the purity of the ethylene are both listed as 99.9% by The Matheson Company. All the data were corrected to 296.6° K. The viscosities of the pure components come from the work of Carr (4). The viscosities of the mixtures are found by using Eq. (38).

The relaxation times for each step in a gas exhibiting double dispersion are found in a way similar to that used for single dispersion. An ideal velocity curve is drawn on a separate sheet and moved along the abscissa over the data until a good fit is observed. For double dispersion however,

Table 3. M_{eff}, η, $1 - \frac{B}{RT}$, K, C_1, $(C_1)_e$, C_2, Θ_1, $(\Theta_1)_e$, Θ_2, $(\nu_1)_e$, $(\nu_2)_e$, $(Z_{10})_1$ and $(Z_{10})_2$ for ethane-ethylene mixtures

% C_2H_6	100	75.1	49.5	25.1	0
M_{eff}	30.070	29.568	29.052	28.558	28.054
$\eta \times 10^2$ cp	0.920	0.948	0.978	1.006	1.036
$1 - \frac{B}{RT}$	0.9919	0.9925	0.9931	0.9936	0.9943
$K \times 10^{-10}$	1.39	1.35	1.31	1.27	1.23
C_1	2.39	2.31	2.24	2.16(5)	2.09
$(C_1)_e$	1.22	0.16	0.32	0.47	0.63
C_2	2.12	1.60	1.05	0.53(5)	—
$\Theta_1 \times 10^8$	1.52	2.05	3.05	6.21	23.4
$(\Theta_1)_e \times 10^9$	7.76	1.39	4.33	13.6	70.5
$\Theta_2 \times 10^9$	1.5	1.4	1.4	2.3	—
$(\nu_1)_e$	821.5	810.3	810.3	810.3	810.3
$(\nu_2)_e$	290	290	290	290	—
$(Z_{10})_1$	100	18	56	169	850
$(Z_{10})_2$	16	14	14	22	—

it is necessary to find the correct relative size of the relaxation times, Θ_1 and Θ_2, by trial and error before a fit can be achieved. The Θ_1 and Θ_2 for the data are then found by taking into account the difference in the abscissa reading (f/p). The change in the relaxation times from the ideal curve values will be inversely proportional to the frequency change necessary to fit the data. The percentage error is determined by varying Θ_1 and Θ_2 to find the limits that will give reasonably good fits on the data. The error in Θ_1 will usually be much less than 10% while the error in Θ_2 is more indefinite but will run, at most, up to 20% error. This method of error determination takes into account all the specific sources of error such as uncertainties in temperature, percentage mixture, wavelength determination, etc.

A careful study of the results listed in Table 3 will show that ethane-ethylene collisions are more effective in energy transfer than ethane-ethane or ethylene-ethylene collisions. The exchange mode for the first step in the ethane curve is the lowest "regular" mode of vibration, 821.5 cm^{-1}. As soon as some ethylene is added to the ethane the exchange mode becomes the lowest mode of vibration of ethylene, 810.3 cm^{-1}. This causes the sharp decrease in $(\Theta_1)_e$ as one goes from 100% ethane to 75.1% ethane. This follows from Eq. (11), which for this case is

$$(\Theta_1)_e = \frac{0.16}{2.31}\,\Theta \quad .$$

$(C_1)_e$ is so small because the exchange mode is in the ethylene molecule and there is only 24.9% present. Hence, also, there is a sharp decrease in $(Z_{10})_1$. It should be made clear that the $(Z_{10})_1$ and $(Z_{10})_2$ reported in Table 3 are collisions per transition for the mixture. The individual components will be considered later.

If one looks at the values of $(\Theta_1)_e$ for the mixtures which have from 0 to 75.1% ethane, there is a gradual decrease. There is a normal decrease expected because the exchange mode is in ethylene and there is a decreasing percentage of ethylene present. The actual decrease in $(\Theta_1)_e$ is greater than this expected decrease as is made very clear by the decreasing Θ_1 and this suggests that ethane-ethylene collisions are more effective in energy transfers than ethylene-ethylene collisions. The collision lifetime for the exchange mode in ethylene, $(Z_{10})_1$, shows a corresponding decrease when the percentage of ethane is increased.

The relaxation times of the second steps in the dispersion curves are not as well known as those for the first steps. Within experimental error one can only be sure that at 25.1% ethane the relaxation time and the collision lifetime is starting to increase. This is expected since there will be many ethylene-ethylene collisions which have no

transitions and thus tend to increase the collision lifetime for the mixture.

The fact that there appears to be a decrease in θ_2 and $(Z_{10})_2$ at 75.1% and 49.5% ethane suggests that the ethylene-ethane collisions are more effective in energy transfer than ethane-ethane collisions. This will be verified when we study the number of collisions suffered by ethane molecules in the mixture per transition. Similar collision lifetimes can be found for ethylene molecules in the mixture.

$1/\theta_2$ is the net number of transitions per second per molecule of the mixture. Therefore, $1/\chi\theta_2$ is the net number of transitions per second per ethane molecule in the mixture and so $\chi\theta_2$ is the relaxation time for an ethane molecule in the mixture with mole fraction χ of ethane present. The collision rates used in Table 3 will be used here also. Any error introduced by this will be negligible because the collision rates of ethane and ethylene are so nearly the same. The results are given in Table 4 where $(Z_{10})_2$ is now the collision lifetime of the hindered mode of rotation of the ethane molecules in the mixture. The $(Z_{10})_2$ in Table 4 is the number of collisions suffered by ethane molecules per transition. One has no doubt here that $(Z_{10})_2$ is decreasing with the addition of more ethylene and therefore, as suggested above, ethylene-ethane collisions are more effective in energy transfers involving the hindered mode of rotation than ethane-ethane collisions.

Table 4. Relaxation times and collision lifetimes of the hindered rotational mode of an ethane molecule in the mixtures

% C_2H_6	$(\chi\theta_2) \times 10^9$	$(Z_{10})_2$
100	1.5	16
75.1	1.1	11
49.5	0.69	7
25.1	0.58	6

By the same argument as above, $(1 - \chi)(\theta_1)_e$ is the relaxation time for the exchange mode of an ethylene molecule in a mixture with mole fraction $(1 - \chi)$ of ethylene. The collision rates used in Table 3 are again used to calculate $(Z_{10})_1$ where $(Z_{10})_1$ is now the number of collisions suffered by ethylene molecules per transition. The results are listed in Table 5.

Table 5 shows that as more ethane is added $(Z_{10})_1$ decreases. Ethane-ethylene collisions are, therefore, much more effective in energy transfers involving the exchange mode of ethylene than ethylene-ethylene collisions.

Table 5. Relaxation times and collision lifetimes of the exchange mode of an ethylene molecule in the mixtures

% C_2H_4	$(1 - \chi)(\theta_1)_e \times 10^9$	$(Z_{10})_1$
100	70.5	850
74.9	10.2	127
50.5	2.2	28
24.9	0.35	5

B. Theoretical Considerations

The double dispersion equation, Eq. (13), has been used for all of the double dispersion cases considered in this work. The interaction terms which enter into the velocity expression when Eq. (13) is used change the velocity curve enough to give a more satisfactory fit on the data than the single dispersion combination results could give. For all of the double dispersion cases studied in this work, Eq. (13) has given good results.

The relation derived for the relaxation times of mixtures is easily tested against experiment and proves to be very satisfactory.

Amme and Legvold (2) have investigated some mixtures that one would expect to obey Eq. (44). A good test of Eq. (44) is to see if $(1/\theta_{AB} + 1/\theta_{BA})$ is really constant for all percentage mixtures of any two given gases. Amme and Legvold (2) studied $CClF_3$ - $CHCl_2F$ mixtures and CF_4 - $CHClF_2$ mixtures. Table 6 shows the results of Eq. (44).

The results for $CClF_3$ - $CHCl_2F$ are very good but the results for CF_4 - $CHClF_2$ are not satisfactory. A look at the work of Amme and Legvold (2) shows that the data for $CClF_3$ - $CHCl_2F$ mixtures is very good but for CF_4 - $CHClF_2$ mixtures more experimental deviations are present. A plot of the percent mixture versus relaxation time should fit a smooth curve. Their data fit a smooth curve better for $CClF_3$ - $CHCl_2F$ than for CF_4 - $CHClF_2$. If one draws a smooth curve through the data for CF_4 - $CHClF_2$ mixtures and then uses points on the curve to calculate $(1/\theta_{AB} + 1/\theta_{BA})$ the results are much better and are shown in Table 6.

McGrath and Ubbelohde (19) report some data on ethylene mixed with various gases. All these mixtures have a very small percentage, χ, of added gas so that the χ^2/θ_{BB} term may be neglected in Eq. (44). Table 7 gives the results of Eq. (44).

Tables 6 and 7 show that $(1/\theta_{AB} + 1/\theta_{BA})$ is indeed constant within experimental error.

Table 6. Values of $(1/\theta_{AB} + 1/\theta_{BA})$ for the mixtures of Amme and Legvold (2)

CCl_3F - $CHCl_2F$		CF_4 - $CHClF_2$		
% CCl_3F	$\left(\frac{1}{\theta_{AB}} + \frac{1}{\theta_{BA}}\right) \times 10^{-8}$	% CF_4	$\left(\frac{1}{\theta_{AB}} + \frac{1}{\theta_{BA}}\right) \times 10^{-8}$	$\left(\frac{1}{\theta_{AB}} + \frac{1}{\theta_{BA}}\right) \times 10^{-8}$
			From raw data	From smooth curve
30	0.210	10	0.211	0.076
50	0.196	30	0.060	0.072
70	0.214	50	0.048	0.069
90	0.203	70	0.071	0.071

Table 7. Values of $\left(\frac{1}{\theta_{AB}} + \frac{1}{\theta_{BA}}\right)$ for the mixtures of McGrath and Ubbelohde (19)

C_2H_4 - neo-pentane		C_2H_4 - cyclo-pentane	
% neo	$\left(\frac{1}{\theta_{AB}} + \frac{1}{\theta_{BA}}\right) \times 10^{-7}$	% cyclo	$\left(\frac{1}{\theta_{AB}} + \frac{1}{\theta_{BA}}\right) \times 10^{-7}$
4.54	10.4	4.23	1.99
2.09	10.2	2.56	0.72
1.14	8.8		

C_2H_4 - cyclo-hexane		C_2H_4 - sulfur hexafluoride	
% cyclo	$\left(\frac{1}{\theta_{AB}} + \frac{1}{\theta_{BA}}\right) \times 10^{-7}$	% sulfur	$\left(\frac{1}{\theta_{AB}} + \frac{1}{\theta_{BA}}\right) \times 10^{-7}$
4.15	12.0	2.54	8.7
3.7	13.3	1.2	8.7

Some data on mixtures have been reported by Miyahara and Richardson (21) which may be used to test Eq. (45). Since others (18, 19, 32) have attempted to use Eq. (41) by assuming that θ_A was the relaxation time calculated from Eq. (10), we will report the results of both equations to show the consistantly better results obtained with Eq. (45). θ_{AB} will be calculated and it should be constant for different percentage mixtures of the same two gases. See Table 8.

Table 8. Values of θ_{AB} for the mixtures of Miyahara and Richardson (21)

Freon 12 - helium			Freon 12 - argon		
% Freon	$\theta_{AB} \times 10^8$ (Eq. (41))	$\theta_{AB} \times 10^8$ (Eq. (45))	% Freon	$\theta_{AB} \times 10^8$ (Eq. (41))	$\theta_{AB} \times 10^8$ (Eq. (45))
18	1.70	0.26	25	0.71	0.16
25	1.45	0.30	49	0.32	0.15
50	1.00	0.39	74	0.37	0.23
76	0.61	0.36			

All these results of experiment are in good agreement and provide strong support for our contention that Eq. (44) is the basic equation to be applied in the study of the relaxation times of binary mixtures.

The relaxation times for the ethane-ethylene mixtures studied here may also be used to test Eq. (44) and Eq. (45).

The first step in the double dispersion curves may be considered as the result of a mixture of ethylene with its vibrational specific heat and ethane with a vibrational specific heat due to its "regular" vibrations. The θ_1's listed in Table 3 are the relaxation times to be used and should yield a constant value for $(1/\theta_{AB} + 1/\theta_{BA})$ in Eq. (44). The results are shown in Table 9.

Table 9. Values of $(1/\theta_{AB} + 1/\theta_{BA})$ for the first step in the double dispersion curves for ethane-ethylene mixtures

% C_2H_6	$\left(\frac{1}{\theta_{AB}} + \frac{1}{\theta_{BA}}\right) \times 10^{-8}$
75.1	0.61
49.5	0.62
25.1	0.51

Table 10. Θ_{AB} for the mode of hindered rotation of ethane in ethane-ethylene mixtures

% C_2H_6	$\Theta_{AB} \times 10^9$
75.1	0.55
49.5	0.45
25.1	0.48

The second step in the double dispersion curves may be considered as a mixture of one gas which has velocity dispersion and one which does not. Eq. (45) is then used to calculate Θ_{AB}, the relaxation time of the mode of hindered rotation of a single ethane molecule in otherwise pure ethylene. The results are shown in Table 10.

The average value of Θ_{AB} is 0.49×10^{-9} seconds which is about 1/3 of Θ_{AA} which is 1.5×10^{-9} seconds. With an error much less than the experimental error in Θ_{AB}, it can be said that the collision rate of an ethane molecule in otherwise pure ethylene, K_{AB}, is the same as the collision rate for pure ethylene. Therefore, the collision lifetime, $(Z_{10})_2^{AB}$ is 4.6 collisions suffered by the ethane molecule per transition. This is compared to 16 collisions per transition when only ethane-ethane collisions are responsible. Thus ethylene-ethane collisions are 3 to 4 times

more effective in energy transfers from the mode of hindered rotation than ethane-ethane collisions.

The results in Table 9 and in Table 10 are constant within experimental error. The results of Eq. (44) and Eq. (45) have been consistently good for all cases tested.

The quantum mechanical prediction of collision lifetimes for molecules of the complexity of those studied here is not feasible. No attempt to use this approach has been made in this work.

V. CONCLUSIONS

1. The ethane derivatives examined all show single dispersion. Pure ethane exhibits double dispersion because of the wide gap in frequency between the lowest mode of vibration and the next lowest mode.

2. The ethane derivatives should be examined by using the lowest "regular" mode of vibration as the exchange mode. The heat capacity of a "regular" mode of vibration will lag at a lower frequency sound wave than the heat capacity of a mode of hindered rotation even if the "regular" mode has a much higher frequency. The single dispersion in the ethane derivatives then requires fairly strong coupling between the "regular" vibrations and the mode of hindered rotation.

3. The double dispersion velocity equation, Eq. (13), gives very good results for all double dispersions studied here. The fairly strong interaction between the relaxation phenomena for each step is clearly brought out by Eq. (13).

4. The relation, Eq. (44), for relaxation times of mixtures proved consistently good.

5. In the de-excitation of the mode of hindered rotation in ethane, ethylene-ethane collisions are 3 to 4 times more effective than ethane-ethane collisions.

VI. BIBLIOGRAPHY

1. Amme, R. C. Temperature dependence of sound dispersion in halo-methane gases. Unpublished Ph.D. thesis. Ames, Iowa, Library, Iowa State University of Science and Technology (1958).

2. Amme, R. and Legvold, S. Sound dispersion in halo-methane mixtures. J. Chem. Phys. 26, 514 (1956).

3. Arnett, R. L. and Crawford, B. L. Vibrational frequencies of ethylene. J. Chem. Phys. 18, 118 (1950).

4. Carr, N. L. Viscosities of natural gas components and mixtures. Institute of Gas Technology Research Bulletin 23, 1 (1953).

5. Daasch, L. W., Liang, C. Y. and Nielsen, J. R. Vibrational spectra and calculated thermodynamic properties of ethyl chloride and 1,1-dichloroethane. J. Chem. Phys. 22, 1293 (1954).

6. Dwyer, R. J. Persistence of molecular vibration in collisions. J. Chem. Phys. 7, 40 (1939).

7. Fowler, R. and Guggenheim, E. A. Statistical thermodynamics. Cambridge, University Press (1949).

8. Glockler, G. and Edgell, W. F. Fundamental frequencies of certain halomethanes. II. The raman spectrum of Fluoroform. J. Chem. Phys. 9, 224 (1941).

9. Herzfeld, K. F. and Litovitz, T. A. Absorption and dispersion of ultrasonic waves. Pure and Applied Physics 7. New York, Academic Press (1959).

10. Herzfeld, K. F. and Rice, F. O. Dispersion and absorption of high frequency sound waves. Phys. Rev. 31, 691 (1928).

11. Jackson, J. M. and Mott, N. F. Energy exchange between inert gas atoms and a solid surface. Proc. Roy. Soc. A 137, 703 (1932).

12. Jeans, J. H. Dynamical theory of gases, 2nd edition. Cambridge, University Press (1916).

13. Kallmann, H. and London, F. Über quantenmechanische Energieübertragung zwischen atomaren systemen. Z. Physik. Chem. B.2, 207 (1929).

14. Kennard, E. H. Kinetic theory of gases. New York, McGraw-Hill Book Company, Inc. (1938).

15. Lambert, J. D. and Salter, R. Vibrational relaxation in gases. Proc. Roy. Soc. A 253, 277 (1959).

16. Landau, L. and Teller, E. Zur theorie der schall dispersion. Phys. Z. der Sowjet. 10, 34 (1936).

17. Licht, W. and Stechert, D. G. Variation of the viscosity of gases and vapors with temperature. J. Phys. Chem. 48, 23 (1944).

18. McCoubrey, J. C., Parke, J. B. and Ubbelohde, A. R. Studies on the transfer of vibrational energy in hydrocarbons. Proc. Roy. Soc. A 223, 155 (1954).

19. McGrath, W. D. and Ubbelohde, A. R. The influence of molecular flexibility on the transfer of vibrational energy in hydrocarbons. Proc. Roy. Soc. A 227, 1 (1954).

20. Meissner, H. P. and Redding, E. M. Prediction of physical constants. Ind. Eng. Chem. 34, 521 (1942).

21. Miyahara, Y. and Richardson, E. G. Ultrasonic relaxation in freon vapors. J. Acoust. Soc. Am. 28, 1016 (1956).

22. Pierce, G. W. Piezoelectric crystal oscillators applied to the precision measurement of the velocity of sound in air and CO_2 at high frequencies. Proc. Am. Acad. Arts and Sciences 60, 271 (1925).

23. Rice, O. K. On collision problems involving large interactions. Phys. Rev. 38, 1943 (1931).

24. Richards, W. T. Supersonic phenomena. Rev. Mod. Phys. 11, 36 (1939).

25. Richardson, E. G. Absorption and velocity of sound in vapors. Rev. Mod. Phys. 27, 15 (1955).

26. Richardson, E. G. Ultrasonic physics. Amsterdam, Elsevier Publishing Company (1952).

27. Rossing, T. D. Oscillator for acoustic interferometry. Unpublished M. S. Thesis. Ames, Iowa, Library, Iowa State University of Science and Technology (1952).

28. Rossing, T. D. Sound dispersion in halogen-substituted methanes. Unpublished Ph.D. Thesis. Ames, Iowa, Library, Iowa State University of Science and Technology (1954).

29. Schwartz, R. N. and Herzfeld, K. F. Vibrational relaxation times in gases (three-dimensional treatment). J. Chem. Phys. 22, 767 (1954).

30. Schwartz, R. N., Slawsky, Z. I. and Herzfeld, K. F. Calculation of vibrational relaxation times in gases. J. Chem. Phys. 20, 1591 (1952).

31. Sette, D., Busala, A. and Hubbard, J. C. Energy transfer by collision in vapors of chlorinated methanes. J. Chem. Phys. 23, 787 (1955).

32. Sette, D. and Hubbard, J. C. Note on thermal relaxation of CO_2 in presence of H_2O and D_2O molecules. J. Acoust. Soc. Am. 25, 994 (1953).

33. Smith, L. G. Infra-red spectrum of C_2H_6. J. Chem. Phys. 17, 139 (1949).

34. Smith, D. C., Brown, G. M., Nielsen, J. R., Smith, R. M. and Liang, C. Y. Infrared and raman spectra of fluorinated ethanes. III. The series CH_3-CF_3, CH_3-CF_2Cl, CH_3-$CFCl_2$, and CH_3-CCl_3. J. Chem. Phys. 20, 473 (1952).

35. Smith, D. C., Saunders, R. A. and Nielsen, J. R. Infrared and raman spectra of fluorinated ethanes. IV. The series CH_3-CH_3, CH_3-CH_2F, CH_3-CHF_2 and CH_3-CF_3. J. Chem. Phys. 20, 847 (1952).

36. Tanczos, F. I. Calculation of vibrational relaxation times of the chloromethanes. J. Chem. Phys. 25, 439 (1956).

37. Walker, R. A. Interpretation of relaxation time measurements in gas mixtures. J. Chem. Phys. 19, 494 (1951).

38. Wilson, E. B., Jr. Present status of the statistical method of calculating thermodynamic functions. Chem. Rev. 27, 17 (1940).

39. Zener, C. Low velocity inelastic collisions. Phys. Rev. 38, 277 (1931).

40. Zener, C. Some observations on the theory of interchange of vibrational and translational energy. Proc. Cambridge Phil. Soc. 29, 136 (1933).

VII. ACKNOWLEDGMENTS

The author wishes to express his gratitude to Dr. Sam Legvold for his guidance. Also, thanks are due Mr. John Olson and Mr. Donald Bell for their help in taking data and making calculations.

We wish to express our gratitude to the Office of Scientific Research of the Air Research and Development Command, United States Air Force, whose support made this work possible.